

DTIC FILE COPY

(2)

AD-A217 261



WRDC-TR-89-2065

AN ELECTROCHEMICAL AND SPECTROSCOPIC  
STUDY OF ELECTRODE PROCESSES

Robert G. Keil  
University of Dayton  
300 College Park  
Dayton, Ohio 45469

June, 1989

Final Report for Period May 1987 - March 1989

Approved for public release; distribution unlimited

DTIC  
ELECTED  
JAN 29 1990  
S B D

Aero Propulsion and Power Laboratory  
Wright Research and Development Center  
Air Force Systems Command  
Wright-Patterson Air Force Base, Ohio 45433-6563

90 01 29 024

**REPORT DOCUMENTATION PAGE**

1a. REPORT SECURITY CLASSIFICATION Unclassified		1b. RESTRICTIVE MARKINGS None										
2a. SECURITY CLASSIFICATION AUTHORITY N/A		3. DISTRIBUTION/AVAILABILITY OF REPORT Approved for public release; distribution is unlimited										
2b. DECLASSIFICATION/DOWNGRADING SCHEDULE N/A												
4. PERFORMING ORGANIZATION REPORT NUMBER(S)  UDR-TR-89-33		5. MONITORING ORGANIZATION REPORT NUMBER(S)  WRDC-TR-89-2065										
6a. NAME OF PERFORMING ORGANIZATION University of Dayton Research Institute	6b. OFFICE SYMBOL (If applicable)	7a. NAME OF MONITORING ORGANIZATION (WRDC/POOS-2) Aero Propulsion and Power Laboratory Wright Research and Development Center										
6c. ADDRESS (City, State, and ZIP Code)  300 College Park Dayton, Ohio 45469-0001	7b. ADDRESS (City, State, and ZIP Code)  Wright-Patterson AFB, Ohio 45433-6563											
8a. NAME OF FUNDING/SPONSORING ORGANIZATION Wright Research and Development Center	8b. OFFICE SYMBOL (If applicable)	9. PROCUREMENT INSTRUMENT IDENTIFICATION NUMBER  F33615-87-C-2712										
8c. ADDRESS (City, State, and ZIP Code)  Wright-Patterson AFB, Ohio 45433-6563	10. SOURCE OF FUNDING NUMBERS  <table border="1"><tr><th>PROGRAM ELEMENT NO.</th><th>PROJECT NO.</th><th>TASK NO.</th><th>WORK UNIT ACCESSION NO.</th></tr><tr><td>61102F</td><td>2303</td><td>S4</td><td>09</td></tr></table>			PROGRAM ELEMENT NO.	PROJECT NO.	TASK NO.	WORK UNIT ACCESSION NO.	61102F	2303	S4	09	
PROGRAM ELEMENT NO.	PROJECT NO.	TASK NO.	WORK UNIT ACCESSION NO.									
61102F	2303	S4	09									
11. TITLE (Include Security Classification)  An Electrochemical and Spectroscopic Study of Electrode Processes												
12. PERSONAL AUTHOR(S) Keil, Robert G.												
13a. TYPE OF REPORT Final	13b. TIME COVERED FROM May 87 TO Mar 89	14. DATE OF REPORT (Year, Month, Day) June 1989	15. PAGE COUNT 49									
16. SUPPLEMENTARY NOTATION												
17. COSATI CODES <table border="1"><tr><th>FIELD</th><th>GROUP</th><th>SUB-GROUP</th></tr><tr><td>10</td><td>02</td><td></td></tr><tr><td>10</td><td>03</td><td></td></tr></table>		FIELD	GROUP	SUB-GROUP	10	02		10	03		18. SUBJECT TERMS (Continue on reverse if necessary and identify by block number)  Melts, Lithium, Non Aqueous, Imidazolium, Spectroscopy	
FIELD	GROUP	SUB-GROUP										
10	02											
10	03											
19. ABSTRACT (Continue on reverse if necessary and identify by block number)  Research on the chloroaluminate melt, methyl-ethyl-imidazolium chloride-aluminum chloride has been conducted to elucidate the structural properties of the melt. The melt was studied by obtaining its fluorescence spectra, NMR spectra and its conductance properties. In addition, ab-initio calculations (Extended Huckel M.O.) on the dichloro-hydrogen species were made. In other solution studies, proton NMR, infrared and Raman spectroscopic studies of the lithium-water interactions in acetonitrile were continued. The hydration number for lithium ion (four) and the oxygen symmetry, $T_d$ , were determined. A gas chromatographic study of the reactivity of lithium with acetonitrile was conducted.												
20. DISTRIBUTION/AVAILABILITY OF ABSTRACT <input checked="" type="checkbox"/> UNCLASSIFIED/UNLIMITED <input type="checkbox"/> SAME AS RPT <input type="checkbox"/> DTIC USERS		21. ABSTRACT SECURITY CLASSIFICATION Unclassified										
22a. NAME OF RESPONSIBLE INDIVIDUAL Richard A. Marsh		22b. TELEPHONE (Include Area Code) (513) 255-7770	22c. OFFICE SYMBOL WRDC/POOS-2									

## TABLE OF CONTENTS

<u>SECTION</u>		<u>PAGE</u>
1	RESEARCH RELATED TO THE CHLOROALUMINATE (MEIC-AlCl <sub>3</sub> ) MELT	1
1.0	Introduction	1
1.1	Investigation of the Fluorescence Spectra of the (MEIC-AlCl <sub>3</sub> ) Melt	1
1.2	Steady-State Spectra	1
1.3	Fluroescence Lifetimes	10
1.4	Conducto-Tensimetric Titration of 0.305 Basic Chloroaluminate Melt and the Presence of the Dechlorohydrogen(I) Species Within the Melt	14
1.5	NMR Studies on the Ternary MEIC-AlCl <sub>3</sub> -HCl System	20
1.6	Temperature Dependent Conductance Measurements	22
1.7	<u>Ab-Initio</u> Molecular Orbital Calculation of Dichlorohydrogen(I) Species	22
2	PROTON NUCLEAR MAGNETIC RESONANCE AND RAMAN SPECTROSCOPIC STUDIES OF LITHIUM-WATER INTERACTIONS IN ACETONITRILE SOLUTIONS	27
2.0	Introduction	27
2.1	Experimental	27
2.1.1	Materials	27
2.1.2	Instrumental Methods	28
2.2	Results and Discussion	29
2.2.1	Proton Nuclear Magnetic Resonance	29
2.2.2	Raman Spectroscopy	30
2.2.3	Infrared Spectroscopy	30
2.3	Summary and Conclusions	31
2.4	References	34



29    
 32    
 34    
 34    
 36    
 . and/or   
 Special

TABLE OF CONTENTS  
(Continued)

<u>SECTION</u>		<u>PAGE</u>
3	A GAS CHROMATOGRAPHIC STUDY OF THE REACTIVITY OF LITHIUM WITH ACETONITRILE	37
3.0	Introduction	37
3.1	Experimental	38
3.2	Results	38
3.3	Conclusions	45
3.4	References	45

## LIST OF ILLUSTRATIONS

### SECTION 1

<u>FIGURE</u>		<u>PAGE</u>	
1	UV/VIS Spectra of MEIC-AlCl <sub>3</sub> Melts Containing Various Mole Fractions(N) of AlCl <sub>3</sub> .	2	
2	Steady State Emission Spectra of the Melts Having Various AlCl <sub>3</sub> Mole Ratios (N=0.33 to 0.66), Excitation Wavelength 340 nm.	4	
3	Steady State Emission Spectra of the Melts Having Various AlCl <sub>3</sub> Mole Ratios (N=0.33 to 0.66), Excitation Wavelength 360 nm.	5	
4	Steady State Emission Spectra of the Melts Having Various AlCl <sub>3</sub> Mole Ratios (N=0.33 to 0.66), Excitation Wavelength 270 nm.	6	
5	Excitation Spectrum of MEIC-AlCl <sub>3</sub> Chloroaluminate Melts		
	(a) N=0.3345	(c) N=0.4501	
	(b) N=0.4005	(d) N=0.5000	7
6	Excitation Spectrum of MEIC-AlCl <sub>3</sub> Chloroaluminate Melts		
	(a) N=0.5503	(c) N=0.6500	
	(b) N=0.6013	(d) N=0.6565	8
7	Phase Recolved Emission Spectra (PRS) of 0.33 Melt (a) nulled at 520nm, (b) nulled at 300 nm.	15	
8	Simulated Spectrum Using $\tau_1=2$ and $\tau_2=7.5$ nsec and a Comparison with the Steady State Emission Spectrum of 0.33 Melt. Excitation Wavelength = 270 nm.	18	
9	A Conducto-Tensimetric Titration of a 0.395 MEIC-AlCl <sub>3</sub> Melt with Dry Gaseous HCl. (a) Tensimetric data, (b) Conductance data.	19	
10	Proton NMR Spectra of 0.395 MEIC-AlCl <sub>3</sub> Chloroaluminate Melt (a), and (b) Melt Treated with HCl (gas) Showing the Presence of HCl <sub>2</sub> Anion.	21	

LIST OF ILLUSTRATIONS (Continued)

SECTION 1

<u>FIGURE</u>		<u>PAGE</u>
11	Variations of Proton Shifts (PPM) and Intensity Ratio with MELT-HCl Composition. (a) HCl proton, (b) Proton-2, (c) Proton-4,5 of the Imidazolium Ring, (d) Intensity Ratio HCl proton/2-H Ring, and (e) Intensity Ratio 1-H/4,5-H Ring.	23
12	Temperature Dependent Conductance of a 1:2 MELT:HCl Solution.	24
13	Dichlorohydrogen(I) Ion, $\text{HCl}_2^-$ .	26

TABLE

1	Observed Peak Positions in the Excitation Spectra of the MEIC-AlCl <sub>3</sub> Chloroaluminate Melt	9
2	Summary of the Steady State Fluorescence Emission for MEIC-AlCl <sub>3</sub> Chloroaluminate Melts (0.33-0.4)	11
3	Summary of the Steady State Fluorescence Emission for MEIC-AlCl <sub>3</sub> Chloroaluminate Melts (0.45-0.55)	12
4	Summary of the Steady State Fluorescence Emission for MEIC-AlCl <sub>3</sub> Chloroaluminate Melts (0.60-0.66)	13
5	Lifetimes/Scattering Reference	16
6	Analysis of Lifetimes of Fluorophores in 0.33 MEIC-AlCl <sub>3</sub> Melt Using Phase and Modulation at Different Frequencies	17

## LIST OF ILLUSTRATIONS (Continued)

### SECTION 2

<u>FIGURE</u>		<u>PAGE</u>
14	Chemical Shift (Hz) at 60 MHz of Water Protons as a Function of Mole Ratio, Water:Lithium Ion, in Acetonitrile.	31
15	Raman Spectra of Lithium Perchlorate (1.6 Molar) in Acetonitrile: (a) No Added Water, (b) Water:Li <sup>+</sup> Molar Ratio 1.5:1, (c) Water:Li <sup>+</sup> Molar Ratio, 4:1.	33
16	Infrared Spectra of Lithium Perchlorate (1.6 Molar) in Acetonitrile Containing Various Amounts of Water: (a) No Added Water, (b) 5.0 Molar Water, (c) 7.0 Molar Water, (d) No Added Water, No LiClO <sub>4</sub> Neat Acetonitrile.	35

### TABLE

1	Chemical Shift Data for Lithium Perchlorate Solutions in Acetonitrile as a Function of Added Water	30
---	--	----

### SECTION 3

### FIGURE

17	Gas Chromatograms of Acetonitrile: (a) Normal, (b) Attenuated, (c) Spiked with Propionitrile.	39
18	Proposed Mechanism for the Chemical Reaction Between Lithium and Acetonitrile.	43

### TABLE

1	Retention Times of Acetonitrile and Propionitrile	40
2	Area Percentage Values of Those Major Peaks From the Reaction Samples 1, 2, 3, 4	40
3	Retention Times (RT) and Area Percentage (A%) Observed the Day After Reaction Reached Termination	46

SECTION 1  
RESEARCH RELATED TO THE CHLOROALUMINATE ( $\text{MEIC-AlCl}_3$ ) MELT

1.0 INTRODUCTION

Ambient temperature chloroaluminate melts were prepared in the usual manner by mixing  $\text{AlCl}_3$  (anhydrous) and 1-methyl-3-ethylimidazolium chloride (MEIC) in different proportion, so that the mole fraction (N) of  $\text{AlCl}_3$  in the melts varied between 0.33 through 0.66. Several samples of authentic melts were also obtained from F. J. Seiler Research Laboratory, U.S. Air Force Systems Command in Colorado Springs, Colorado.

The work presented in this report may be divided into two categories: (a) Extensive spectrofluorometric studies and determination of the lifetimes of certain species present in the melts, and (b) Modification of the chloroaluminate melt to increase the conductance and variation of conductance with temperature.

1.1 INVESTIGATION OF FLUORESCENCE SPECTRA OF THE ( $\text{MEIC-AlCl}_3$ ) MELT

The UV absorption spectra of the melts varies with the composition parameter 'N' where 'N' is the mole ratio of  $\text{AlCl}_3$  in the melt (Figure 1). We were interested in investigating the fluorescence spectra and lifetimes of these melts and learning more about the nature of the species present, by investigating the lifetimes.

1.2 STEADY-STATE SPECTRA

The fluorescence spectra of organic compounds are greatly influenced by their composition. The steady state emission spectra of a variety of composition (N=0.33 through N=0.66) of  $\text{MEIC-AlCl}_3$  chloroaluminate melts at selected excitations 270nm,

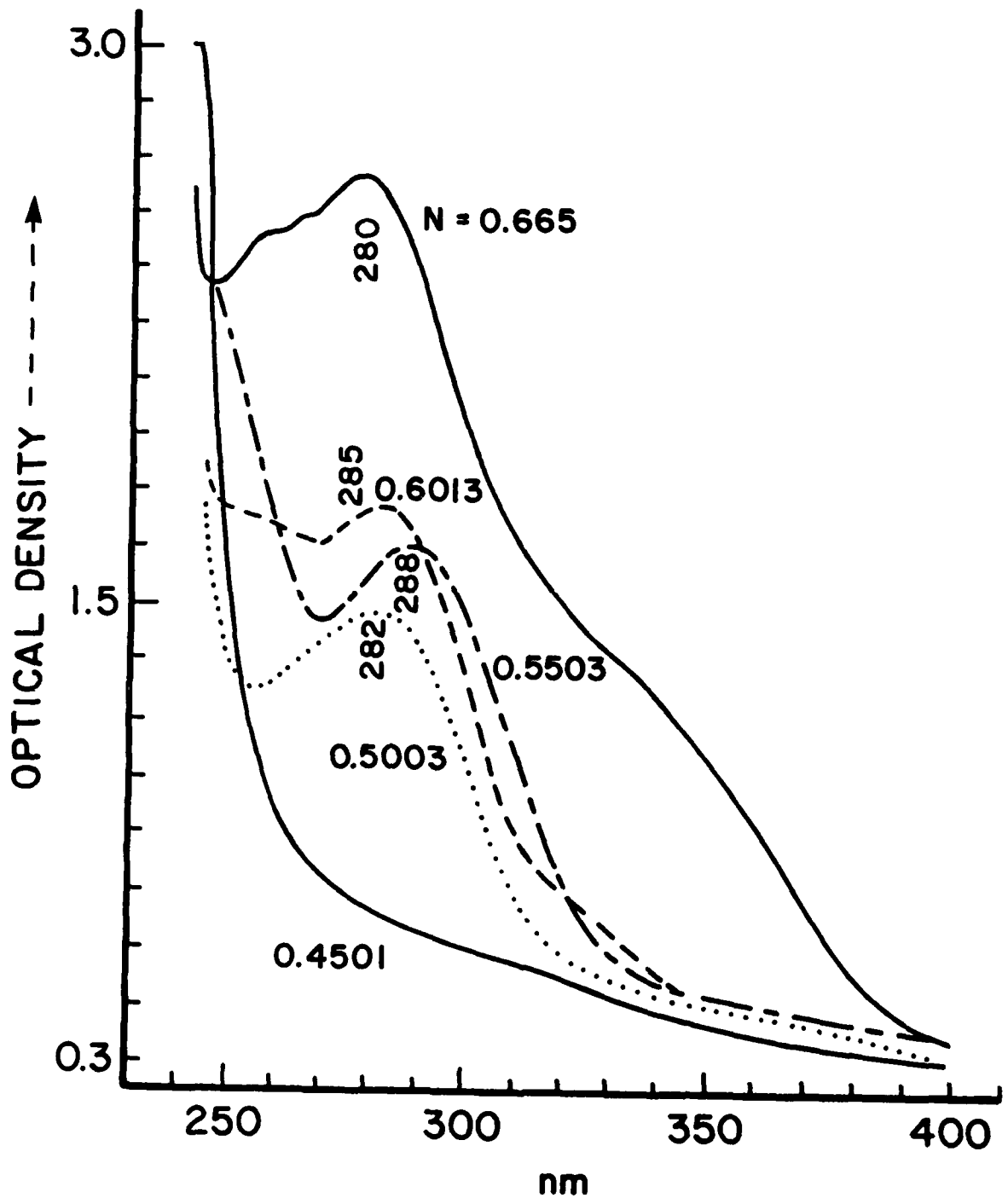


FIGURE 1. UV/VIS SPECTRA OF METC- $\text{AlCl}_3$  MELTS CONTAINING VARIOUS MOLE FRACTION(N) OF  $\text{AlCl}_3$ .

340nm, and 360nm are shown in Figures 2 through 4. It is evident that the spectrum profile varies greatly with the mole fraction of  $\text{AlCl}_3$  present in these melts as well as with the change of excitation wave lengths. These spectra were recorded with a Phase Resolved Spectrofluorometer (Model SLM-4800, SLM-AMINCO Company, Urbana, IL) in the steady state mode.

In order to confirm the results obtained with a Phase Resolved Spectrofluorometer (PRS), we have obtained both excitation and emission spectra using our Perkin-Elmer LS-5 Spectrofluorometer in its steady state mode.

The UV excitation spectra of the MEIC- $\text{AlCl}_3$  melts ( $N=0.3345$  through  $N=0.6665$ ) are reported in Figures 5 and 6, and the major peaks in the excitation spectra are tabulated in Table 1. An analysis of Table 1 and Figures 5 and 6 indicates the presence of two broad and intense peaks around 285 and 360nm region with a weaker sharp peak at 260nm, for the basic and the neutral melts ( $N<0.5$ ). The spectra of the acidic melts having  $N>0.5$  exhibit somewhat simpler excitation spectra having a sharp and intense peak around 245nm (see Table 1).

The results can be explained on the basis of speciation, having imidazolium cation and  $[\text{AlCl}_4]^-$  anion in the basic melts, with some "free" chloride ions for charge neutrality. With the increase in the N-value to 0.5, we have almost neutral melt having equal amount of imidazolium cation and  $[\text{AlCl}_4]^-$  anion and no chloride ion present. With further increase in the n-value, we have to consider at least three different species to be present in the melt, e.g., imidazolium cation,  $[\text{AlCl}_4]^-$  and  $[\text{Al}_2\text{Cl}_7]^-$  anions. The excitation spectra of the melts are compatible with the UV absorption spectra in Figure 1.

The steady state fluorescence spectrum profiles of the melts obtained with the PRS are presented in Figures 2, 3, and 4 using selective excitation wavelengths, 270, 340, and 360nm

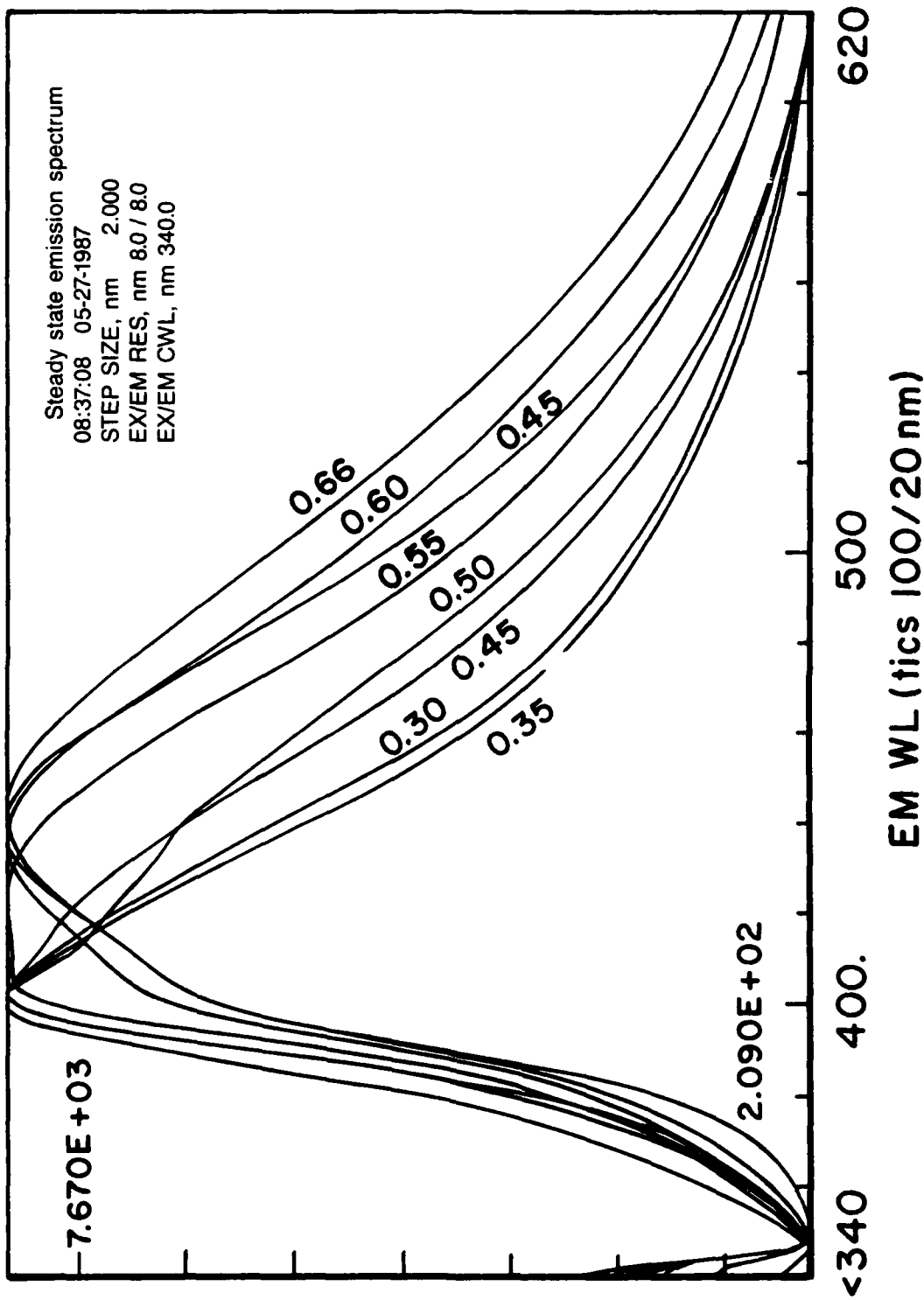


FIGURE 2. STEADY STATE EMISSION SPECTRA OF THE MELTS HAVING VARIOUS  $\text{AlCl}_3$  MOLE RATIOS  
 $(N=0.33 \text{ to } 0.66)$ , EXCITATION WAVELENGTH 340 nm.

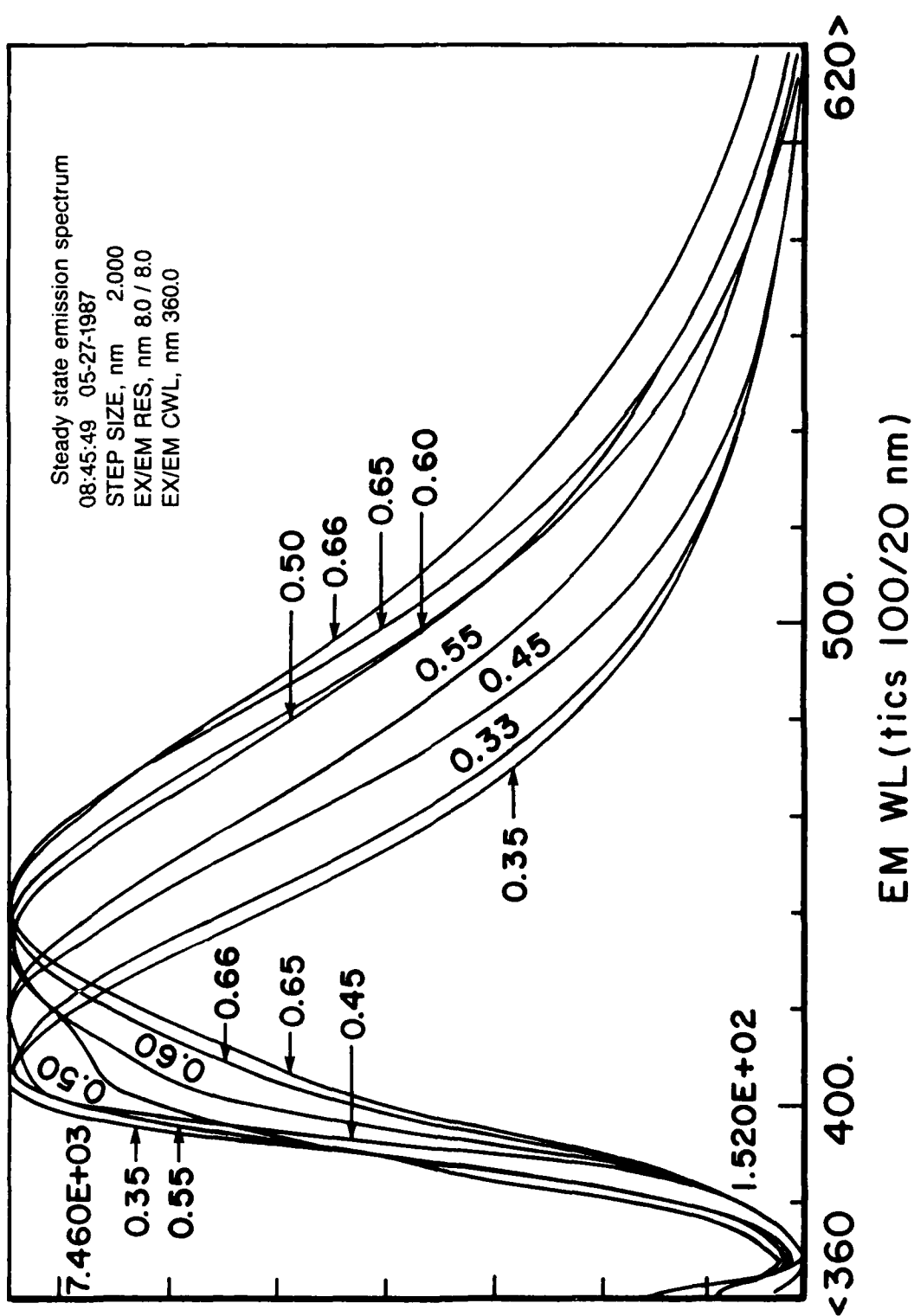


FIGURE 3. STEADY STATE EMISSION SPECTRA OF THE MELTS HAVING VARIOUS  
 $\text{AlCl}_3$  MOLE RATIOS ( $n=0.33$  to  $0.66$ ), EXCITATION WAVELENGTH  
 360 nm.

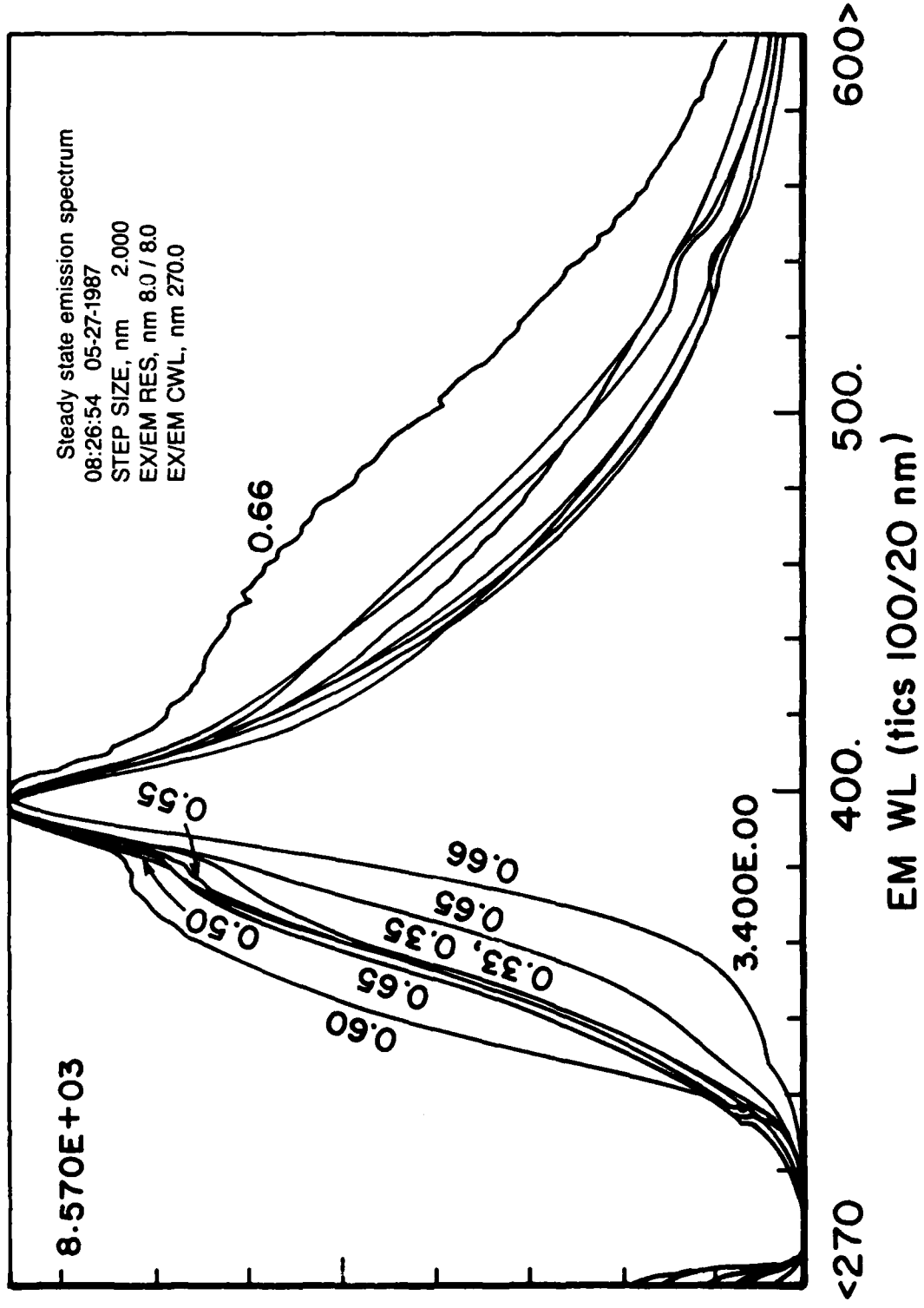


FIGURE 4. STEADY STATE EMISSION SPECTRA OF THE MELTS HAVING VARIOUS  $\text{AlCl}_3$  MOLE RATIOS ( $n=0.33$  to  $0.66$ ), EXCITATION WAVELENGTH 270 nm.

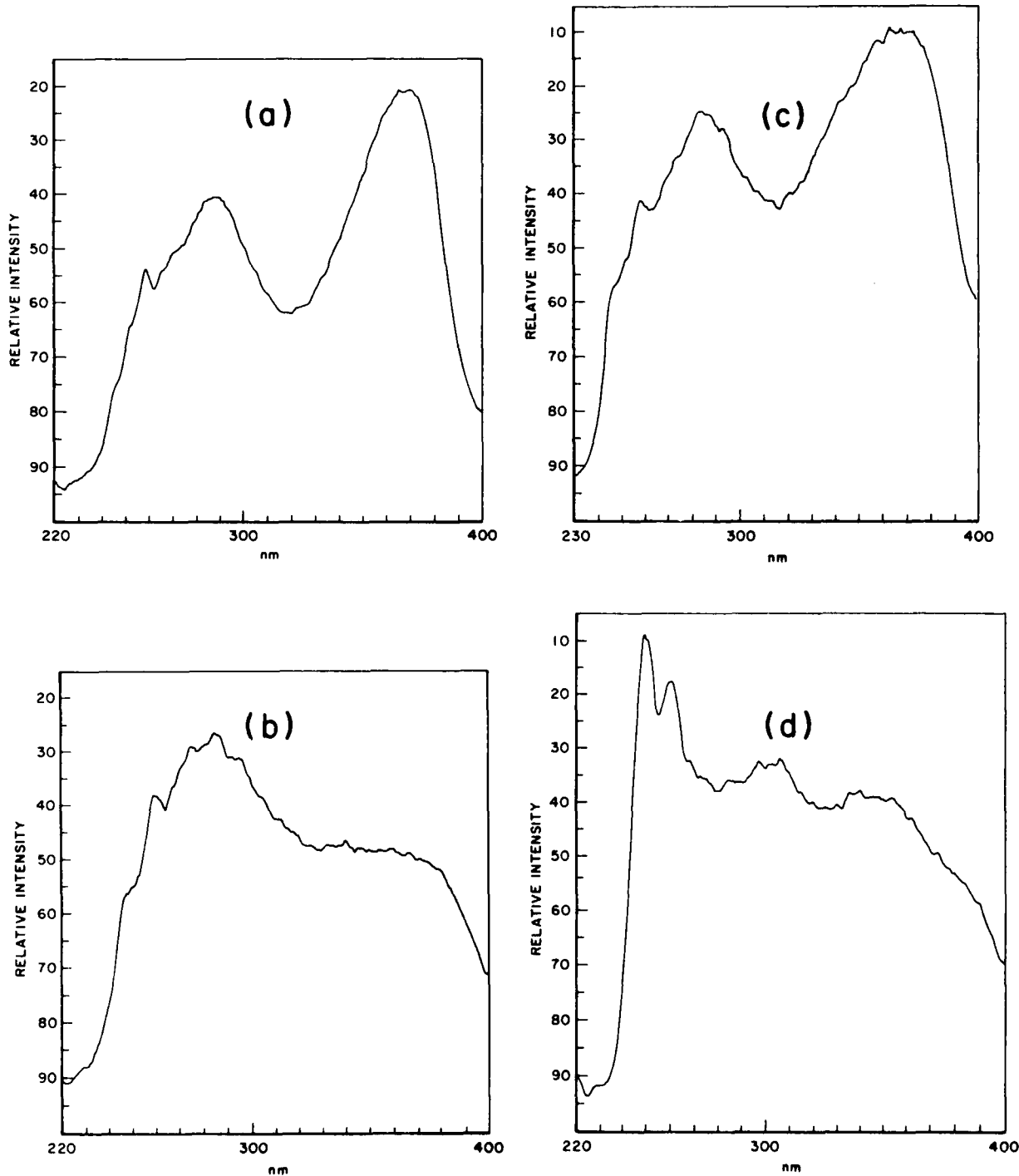


FIGURE 5. EXCITATION SPECTRA OF MEIC- $\text{AlCl}_3$  CHLOROALUMINATE MELTS:  
 (a)  $N=0.3345$ , (b)  $N=0.4005$ , (c)  $N=0.4501$  and (d)  $N=0.5000$ .

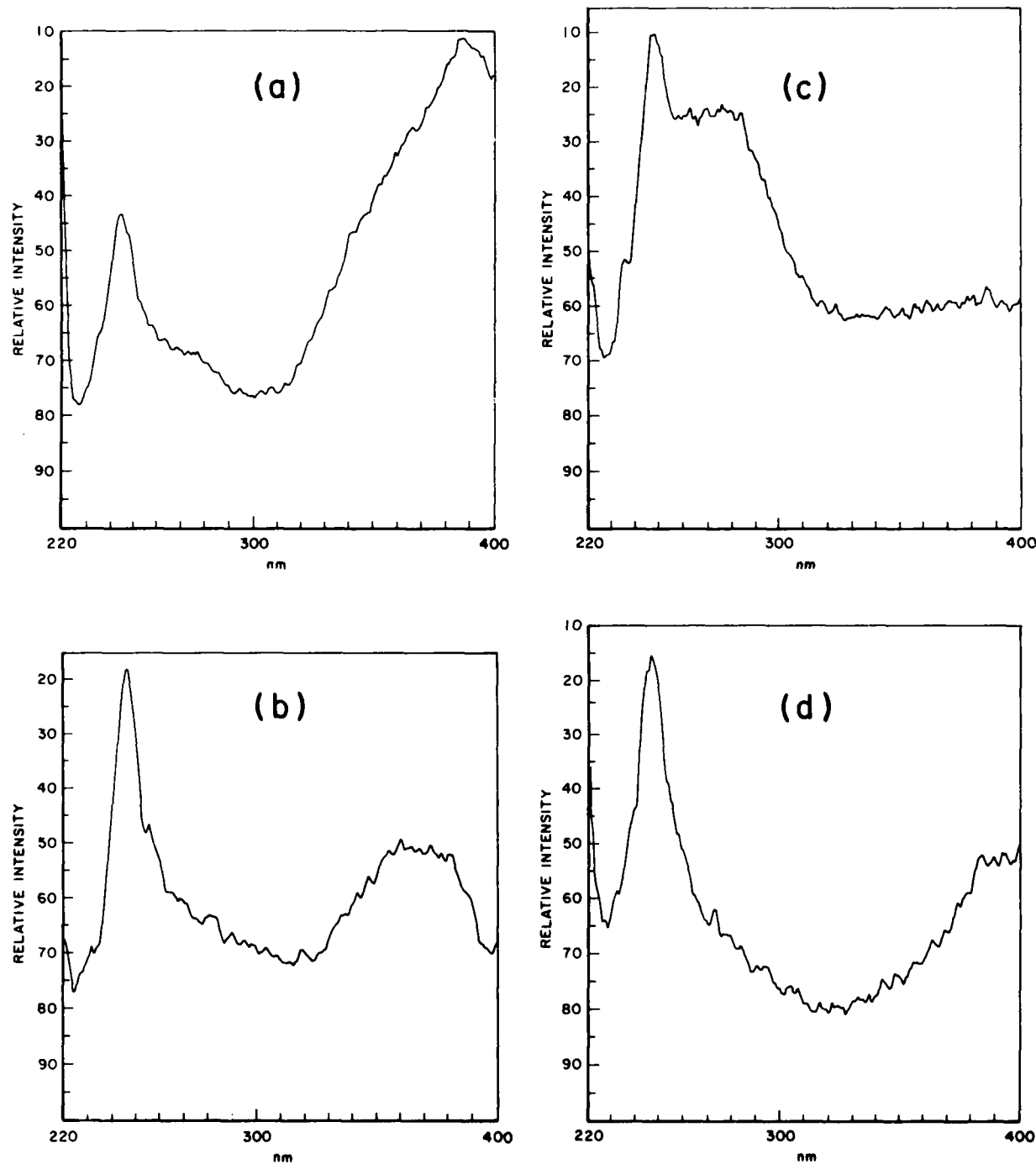


FIGURE 6. EXCITATION SPECTRUM OF MEIC-AlCl<sub>3</sub> CHLOROALUMINATE MELTS:  
 (a) N=0.5503, (b) N=0.6013, (c) N=0.6500, and (d) N=0.6565.

TABLE 1

OBSERVED PEAK POSITIONS IN THE EXCITATION SPECTRA  
OF THE  $\text{MEIC-}\text{AlCl}_3$  CHLOROALUMINATE MELT

MELT (N)	$\lambda_{\text{em}}$ (NM)	EXCITATION MAX. (NM)	SHOULDERS AND OTHER SECONDARY PEAKS
0.3345	420	290, <u>365</u>	260
0.3500	420	258	286, 370
0.4000	420	258, <u>280</u>	250, 370
0.4501	427	285, <u>365</u>	250, 258
0.5000	420	248, <u>260</u>	300, 336, 352
0.5503	430	245, <u>385</u>	270, 345
0.6013	420	245	265, 345(?) , <u>360, 380</u>
0.6500	420	246	
0.6566	420	246	269(?) , 385(?)

respectively. These spectrum profiles correspond well with those obtained with our PE L5-5 pulsed spectrofluorometer working in the steady state mode. A summary of the variation of the emission peak positions of the chloroaluminate melts with excitation wavelengths is presented in Tables 2, 3, and 4. A preliminary analysis of these profiles indicate the presence of more than one fluorescing species in these melts.

### 1.3 FLUORESCENCE LIFETIME

The lifetimes of fluorescence decays are important parameters in identifying the "fluorophores" present in a system. The average lifetime of an organic moiety is of the order of nano or pico seconds. Our LS-5 spectrofluorometer has an instrumental limit of about 10-20 microseconds. Hence, lifetimes shorter than this limit cannot be measured. The methylethylimidazolium cation may exhibit shorter lifetime (a few nano-seconds). This limitation in instrument capability required us to look for an alternate means of measuring the lifetime. SLM-AMINCO company of Urbana, IL, provided their nano-second instrument (SLM-4800), a semi-automatic phase resolved spectrometer, for limited investigation of our melts.

The phase resolved spectrofluorometers operate at a different principal than the conventional flash techniques, and allow the measurement of very short lifetimes. In the phase-resolved technique both phase ( $\phi$ ) and modulation (M) of the emission signals are recorded at different frequencies (typically 6, 18, or 30 MHz) and the lifetime of the species is related by the following relationships:

$$\tau_p = (1/2\pi f) \tan \phi \quad (1)$$

$$\tau_M = (1/2\pi f)(1/M^2 - 1)^{1/2} \quad (2)$$

If the emission is spectrally homogeneous only one exponential decay should be observed with  $\tau_p = \tau_M$ . If  $\tau_p$  and  $\tau_M$  are

TABLE 2  
SUMMARY OF THE STEADY STATE FLUORESCENCE EMISSION  
FOR MEIC- $\text{AlCl}_3$  CHLOROALUMINATE MELTS (0.33-0.4)

MELT (N)	$\lambda$ EXCITATION (NM)	$\lambda_{\text{em}} (\text{NM})$
0.3345	250 270 280 290 340 350 365 390	<u>405</u> , 430 <u>410</u> , ~440 <u>410</u> <u>410</u> <u>420</u> , ~470 (v. broad) <u>420</u> , ~480 <u>425</u> , ~480 <u>440</u> , longtail
0.3500	240 258 270 286 340 360 376 390	398 418 418 418 420 420 425 440
0.4000	250 258 280 355 370 390	<u>415</u> , sh @ 395, 460 <u>455</u> , sh @ 400, 425 <u>450</u> , sh @ 395 <u>455</u> <u>458</u> sh @ 458, 480(?) <u>460</u> sh @ 460, 480(?)

TABLE 3  
SUMMARY OF THE STEADY STATE FLUORESCENCE EMISSION  
FOR MEIC-AlCl<sub>3</sub> CHLOROALUMINATE MELTS (0.45-0.55)

MELT (N)	$\lambda$ EXCITATION (NM)	$\lambda_{eml}$ (NM)
0.4501	240 250 258 270 285 340 365 370 390	400, 430 (broad sh) <u>415</u> , 440 (broad sh) <u>425</u> , 370 sh, 460 sh <u>425</u> 370 sh, 465 sh <u>425</u> , 365 sh, (405(?)), 465 sh <u>425</u> , 480(?) <u>432</u> , 470 sh <u>445</u> , 470 sh(?) <u>450</u>
0.5000	240 250 260 270 280 305 340 355 360 370 390	400 <u>400</u> <u>400</u> , 440 sh(?) <u>400</u> , 315, 430(?) <u>400</u> , 350, 450 sh(?) <u>400</u> , 430 longtail <u>440</u> with longtail <u>445</u> with longtail <u>445</u> with longtail <u>450</u> with longtail <u>455</u> with longtail
0.5503	245 275 340 360 370 380 390 400	<u>410</u> <u>420</u> <u>435</u> <u>432</u> <u>430</u> <u>435</u> <u>435</u> <u>450</u>

TABLE 4  
SUMMARY OF THE STEADY STATE FLUORESCENCE EMISSION  
FOR MEIC-AlCl<sub>3</sub> CHLOROALUMINATE MELTS (0.60-0.66)

MELT (N)	$\lambda$ EXCITATION (NM)	$\lambda_{em1}$ (NM)
0.6013	245 260 270 280 340 350 360 365 380 390	<u>405</u> <u>420</u> <u>415</u> , 485(?) <u>430</u> , 485(?) <u>450</u> , 430 sh, 485(?) <u>448</u> , 410(?) <u>465</u> , 510(br.?) <u>445</u> , 510(br.?) <u>445</u> , 490(?), 520(br.?) <u>450</u> , 520
0.6665	246 250 260 270 280 350 360 380 390	<u>425</u> , 460 sh, 520 sh(?) <u>425</u> , 460 sh, 525 sh(?) <u>420</u> , 460 sh <u>410</u> , 460 (prominant sh) <u>460</u> , 410 sh, 490 sh <u>460</u> <u>460</u> <u>462</u> <u>465</u>

different, then there exists a heterogeneous system with more than one lifetime related to different species in the system.

We have investigated the phase resolved spectra of 0.33 melt (see Figure 7) by nulling at 300 and 520nm. The PRS spectra definitely show the presence of two different phosphors. We have then measured both phase and modulation at frequencies 6, 18, and 30 MHz and collected enough data to have estimates of average  $\tau_p$  and  $\tau_M$  (see Table 5). These data were then statistically analyzed by a specially developed computer program. This heterogeneity analysis finally yielded the actual values of the  $\tau$ 's:  $\tau_1 = 2\text{ns}$  and  $\tau_2 = 7.5\text{ns}$  (see Table 6). Using these two  $\tau$ -values we have simulated the steady state spectrum of 0.33 melt which is shown in Figure 8. A very good fit was obtained.

Summarizing, we have shown that 0.33 melt contains at least two fluorophores having emission maxima at about 400 and about 450nm with fluorescence lifetimes of 2 and 7.5 ns. We believe that the organic MEIC moiety has lifetime of 7.5 ns. The time constraint and the unavailability of PRS on-site have drastically limited our investigation although giving us some valuable insight on the nature of the species.

#### 1.4 CONDUCTO-TENSIMETRIC TITRATION OF 0.395 BASIC CHLOROALUMINATE MELT AND THE PRESENCE OF THE DICHLOROHYDROGEN(I) SPECIES WITHIN THE MELT

The tensimetric titration of basic (0.395) MEIC- $\text{AlCl}_3$  chloroaluminate melt has been extended to include simultaneous measurements of conductivity and the partial pressure (tensimetry) in a specially designed and constructed cell. Dry 0.395 melt was titrated with dry gaseous HCl. Figure 9 shows the results of a conducto-tensimetric titration. It is obvious that the free chloride ion present in the basic (0.395) melt is being titrated. From the break in the tensimetric titration curve (9a) as well as the conductance curve (9b) it is evident that a

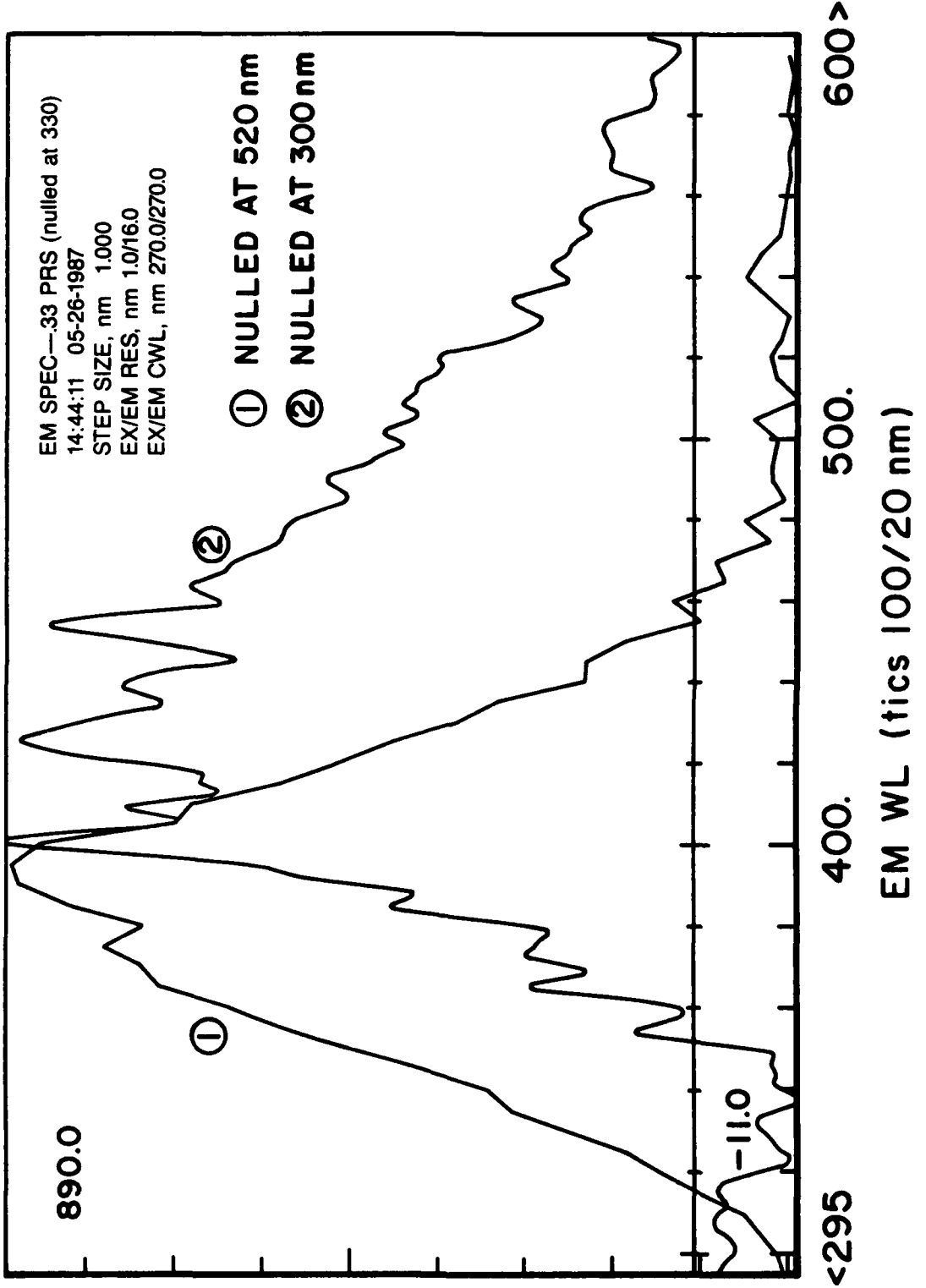


FIGURE 7. PHASE RESOLVED EMISSION SPECTRA (PRS) OF 0.33 MELT (a) NULLED AT 520 nm, AND  
 (b) NULLED AT 300 nm.

TABLE 5

## LIFETIMES/SCATTERING REFERENCE

FREQUENCY = 18.0 Mhz

No.	Lifetimes (ns) Tau-P    Tau-M		Standard Deviation (ns) Phase Mod	Meter Reading Phase Mod
1	---	---	---	---
2	+2.611	+3.103	+0.000/+0.000	+0.000/+0.000
3	+2.621	+3.078	+0.000/+0.000	+0.000/+0.000
4	+2.619	+3.161	+0.005/-0.005	+0.042/-0.043

AVERAGES

No.	Average Tau Tau-M	Standard Deviation (ns) Phase Mod	SAM/REF Phase Mod
4	+2.617	+3.114	+0.005/-0.005    +0.042/-0.043    16.487    0.9432

FREQUENCY = 30.0 Mhz

No.	Lifetimes (ns) Tau-P    Tau-M		Standard Deviation (ns) Phase Mod	Meter Reading Phase Mod
1	---	---	---	---
2	+2.330	+2.963	+0.000/+0.000	+0.000/-0.000
3	+2.331	+2.984	+0.000/+0.000	+0.000/-0.000
4	+2.341	+2.999	+0.006/-0.006	+0.018/-0.018

AVERAGES

No.	Average Tau Tau-M	Standard Deviation (ns) Phase Mod	SAM/REF Phase Mod
4	+2.334	+2.982	+0.006/-0.006    +0.018/-0.018    23.747    0.8717

TABLE 6

ANALYSIS OF LIFETIMES OF FLUOROPHORES IN 0.33 MEIC-AlCl<sub>3</sub>  
MELT USING PHASE AND MODULATION AT DIFFERENT FREQUENCIES

## Heterogeneity Analysis

---

Frequency 1	Tau-Phase	Tau-Mod
18.000	+2.617	+3.114
Frequency 2	Tau-Phase	Tau-Mod
30.000	+2.334	+2.982
Tau-1 = +1.808 nsec	Fractional intensity = +0.779	
Tau-2 = +7.499 nsec	Fractional intensity = +0.221	

---

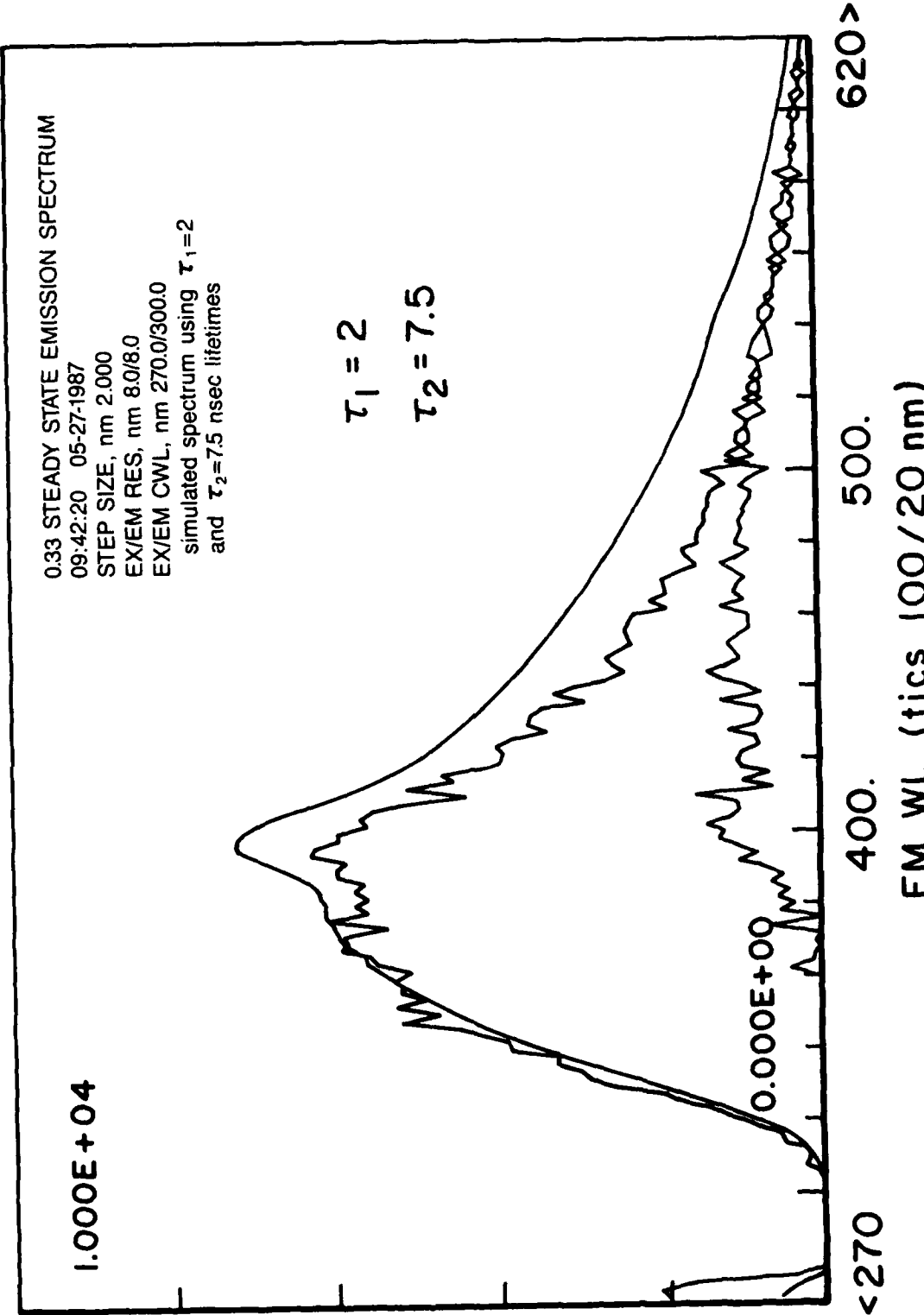


FIGURE 3. SIMULATED SPECTRUM USING  $\tau_1=2$  AND  $\tau_2=7.5$  n sec AND A COMPARISON  
 WITH THE STEADY STATE EMISSION SPECTRUM OF THE 0.33 MELT.  
 EXCITATION WAVELENGTH = 270 nm.

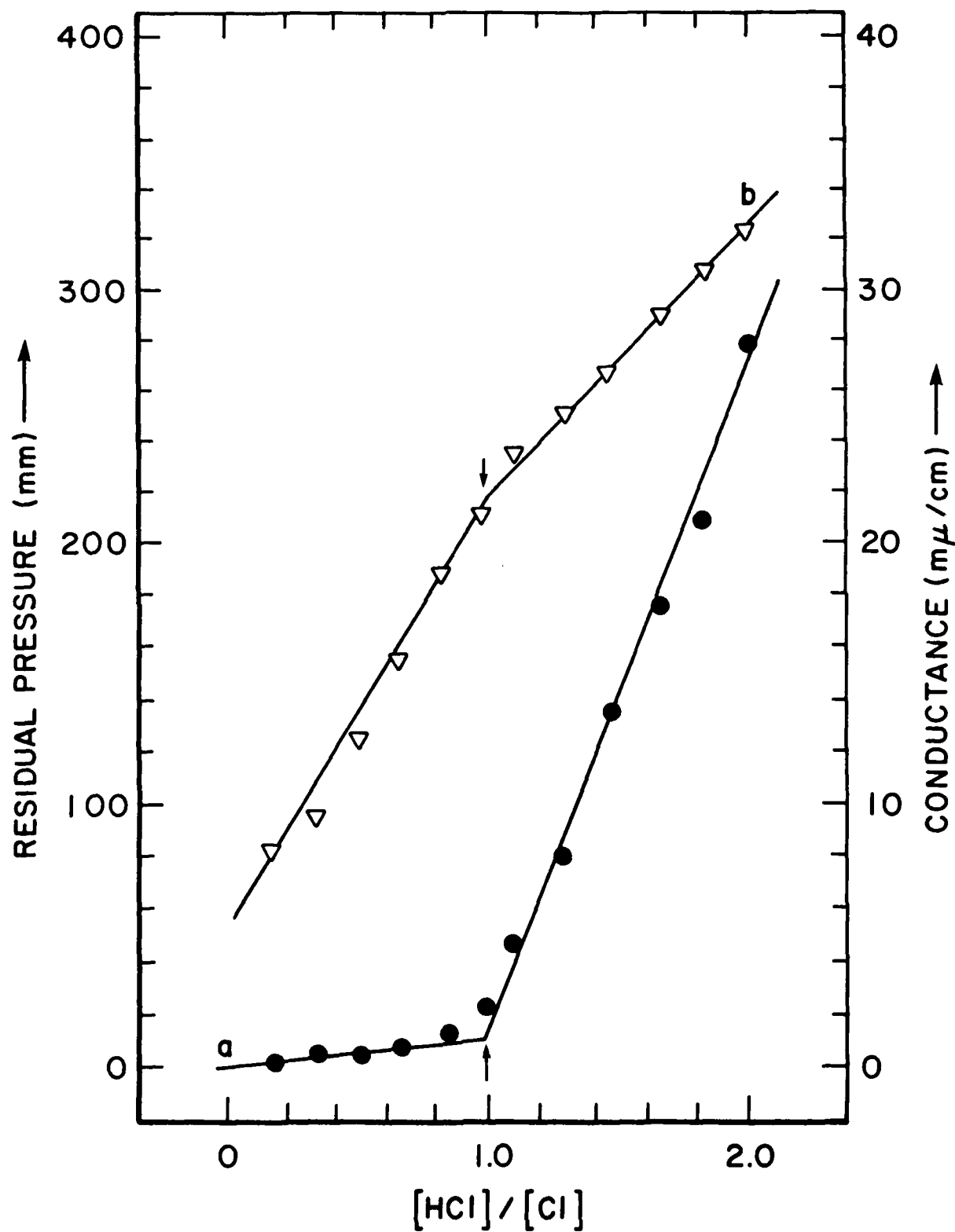


FIGURE 9. A CONDUCTO-TENSIMETRIC TITRATION OF A 0.395 MEIC- $\text{AlCl}_3$  MELT WITH DRY GASEOUS HCl.  
 (a) TENSIMETRIC DATA, (b) CONDUCTANCE DATA

compound of the composition 1:1 ratio of  $[HCl]/[Cl^-]_{\text{FREE}}$  exists in the solution, i.e., melt.



At the Electrochemical Society meeting in October 1987, the tensimetric results were first reported and created some excitement amongst electrochemists as well as inorganic chemists, that a species like  $[HCl_2]^-$  appear to exist in solution under a non-aqueous environment. The dichlorohydrogen(I) species was found to be stable over several months in a closed (sealed) system.

### 1.5 NMR STUDIES ON THE TERNARY MEIC-AlCl<sub>3</sub>-HCl SYSTEM

Figure 10 compares the shifts and the integrated intensities of the H-NMR peaks of a 0.395 MEIC-AlCl<sub>3</sub> melt and the same melt treated with HCl gas and containing  $[HCl_2]^-$  ion. The NMR data may be summarized as follows:

- 2-H Proton: Moved upfield (relatively large shift)  
with respect to the melt, i.e., ELECTRON  
DENSITY HAS INCREASED AROUND 2-H "SHIELDED"
- 4,5-H Protons: Moved upfield, much less than 2-H as  
expected
- H of  $[HCl_2]^-$ : Furthest downfield (12.28 ppm) i.e., the  
ELECTRON DENSITY PREDOMINATELY RESTS ON  
CHLORIDES. The proton is "DESHIELDED"  
(for molecular orbital (M.O.) calculation  
see next section).

A more extensive study of the variations of the proton shifts and intensity ratio with MELT-HCl composition is reported in Figure 11. It is interesting to see that at a low mole ratio of  $[HCl_g]$  and free  $[Cl^-]$ , the  $[HCl_2]^-$  proton shifted more and more downfield until a more ratio of one and then a reverse trend is obtained with increasing mole ratio.

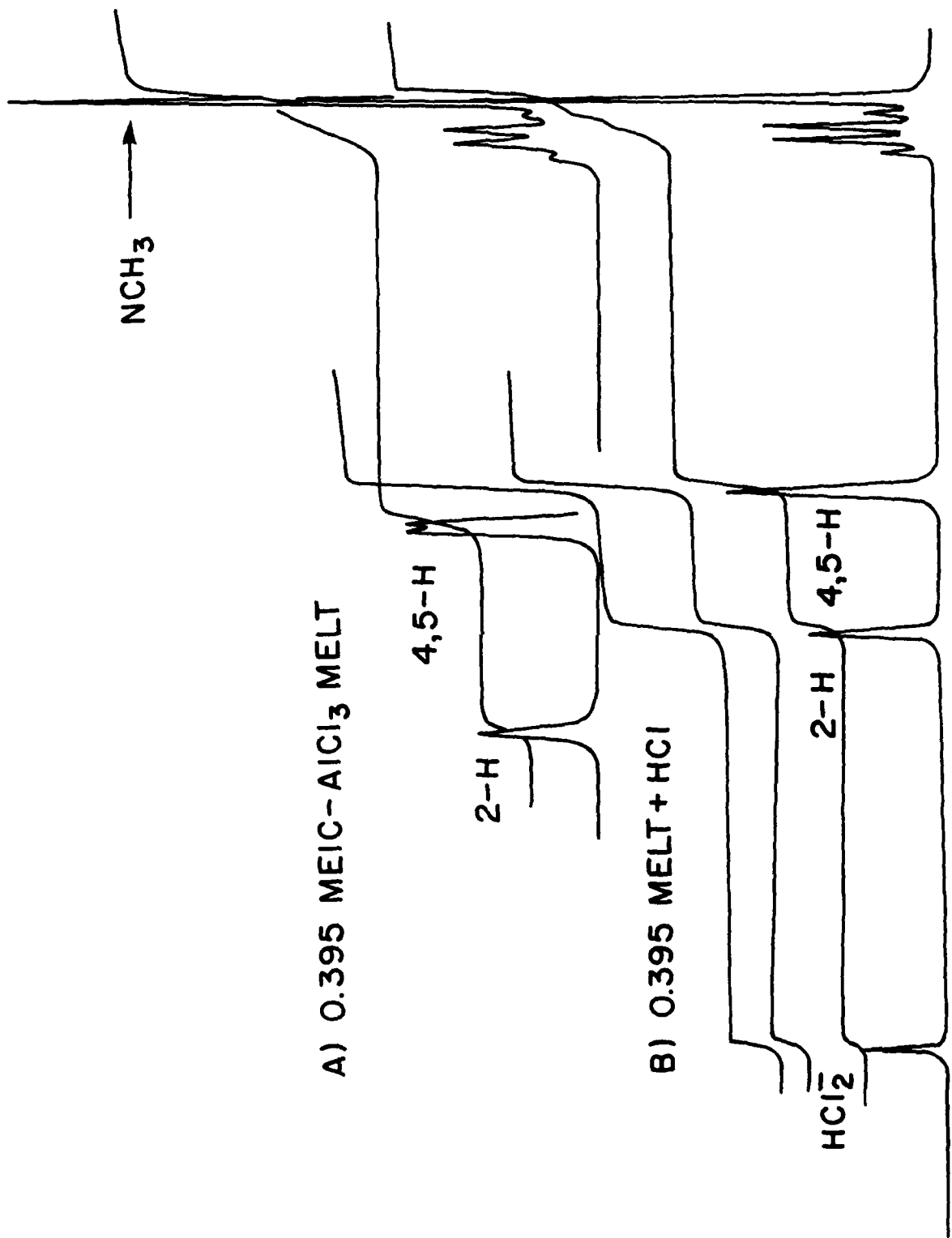


FIGURE 10. PROTON NMR SPECTRA OF 0.395 MEIC- $\text{AlCl}_3$  CHLOROALUMINATE MELT  
 (a); and (b) MELT TREATED WITH HCl GAS SHOWING THE PRESENCE OF  
 $\text{HCl}_2^-$  ANION.

The intensity ratio of [2-H]/[4,5-H] protons of the imidazolium ring is virtually constant over a mole ratio of  $[HCl]:[Cl^-]$  up to two, as expected. This is very significant and strongly indicates that no change of the imidazolium moiety is taking place (substitution or otherwise) with the HCl treatment of the melt. A continuous increase of HCl proton intensity is noticed as more and more  $[HCl_2^-]$  ion is formed, taking 2-H proton intensity as a standard (Figure 11).

#### 1.6 TEMPERATURE DEPENDENT CONDUCTANCE MEASUREMENTS

Preliminary studies on the variation of conductance of the ternary system (MEIC-AlCl<sub>3</sub>-HCl) with temperature were performed at  $[HCl]:[Cl^-]$  mole ratio of 2. Figure 12 presents the conductance versus temperature curve between +30° and -60°C. As expected, the ternary system exhibited the decrease of conductance with temperature. It is interesting that the effective conductivity of the system between -20° and -40°C is about equal to that of the force melt (MEIC-AlCl<sub>3</sub>) without HCl at room temperature. Although the system becomes viscous, it still exhibits enough conductance to be a profitable battery liquid at low temperature (-20° to -60°C).

#### 1.7 AB-INITIO MOLECULAR ORBITAL CALCULATION OF DICHLOROHYDROGEN(I) SPECIES

The hydrogendichloride ion  $[HCl_2^-]$  shows a divalency for the central proton, a species of significant theoretical interest. M.O. calculations on  $[HCl_2^-]$  using a very sophisticated ab-initio procedure involving the use of Hartree-Fock (DZ) wave functions show that the species in question is stabilized by about 28 KCal per mole with respect to its constituents.

In some organic compounds containing  $[HCl_2^-]$  ion, the X-ray analysis showed the anion ( $HCl_2^-$ ) to be somewhat bent ( $\angle Cl-H-Cl = 168^\circ$ ) with unequal H-Cl bond distances (1.45 and 1.78 Å). Our

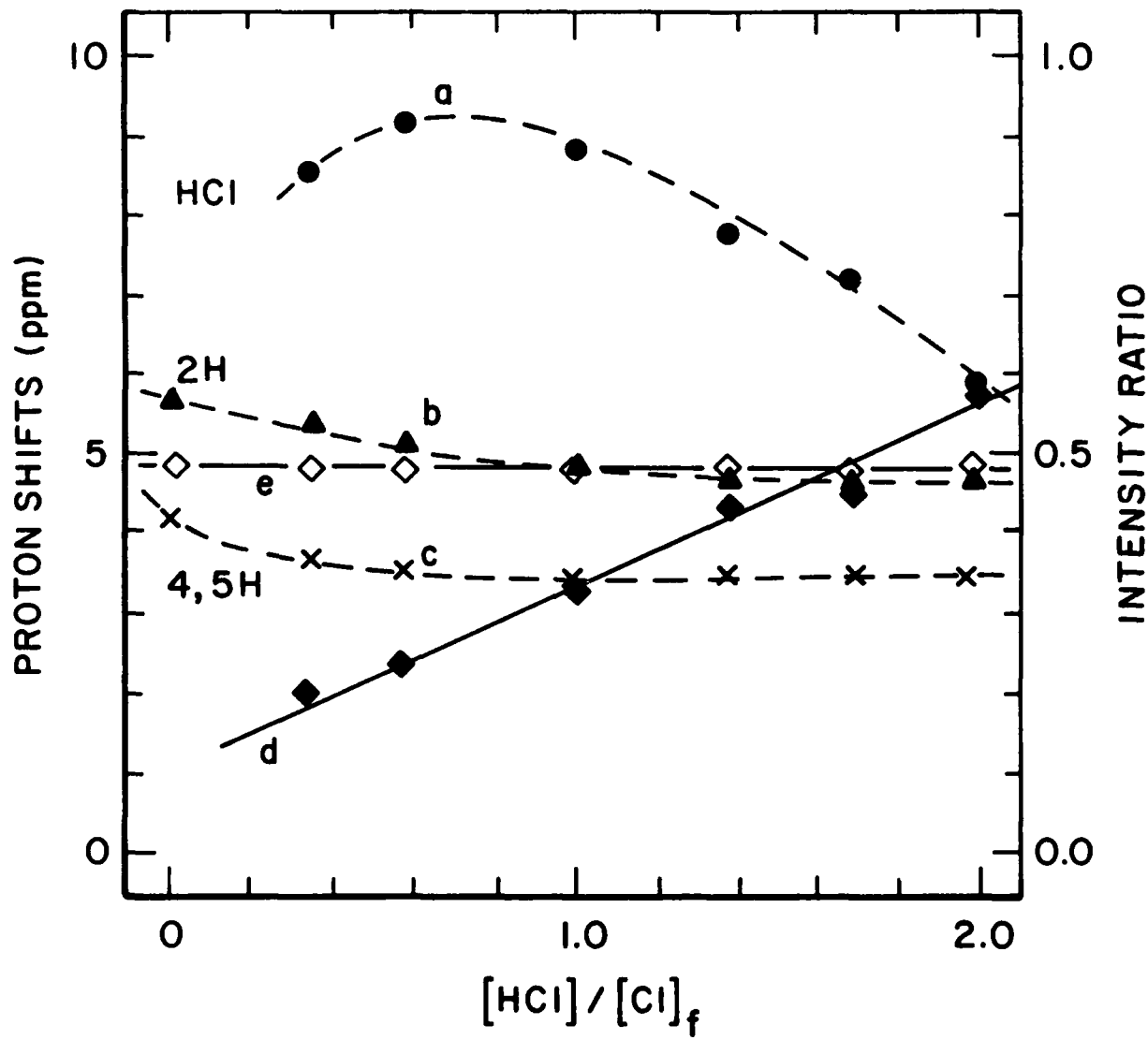


FIGURE 11. VARIATIONS OF PROTON SHIFTS (PPM) AND INTENSITY RATIO WITH MELT-HCl COMPOSITION.  
 (a) HCl PROTON; (b) PROTON-2; (c) PROTON-4,5 OF THE IMIDAZOLIUM RING; (d) INTENSITY RATIO HCl PROTON/2-H RING, AND (e) INTENSITY RATIO 1-H/4,5-H RING.

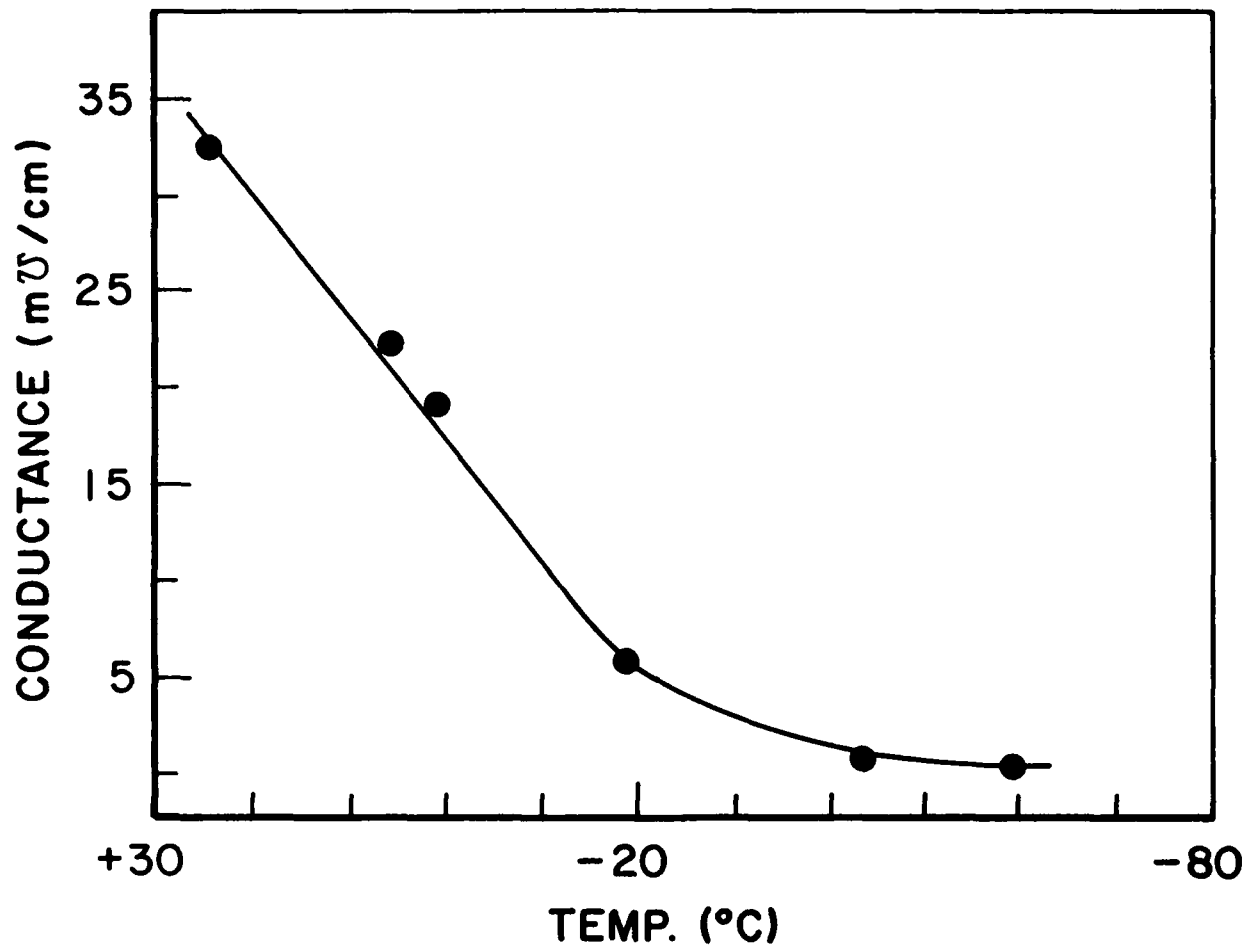
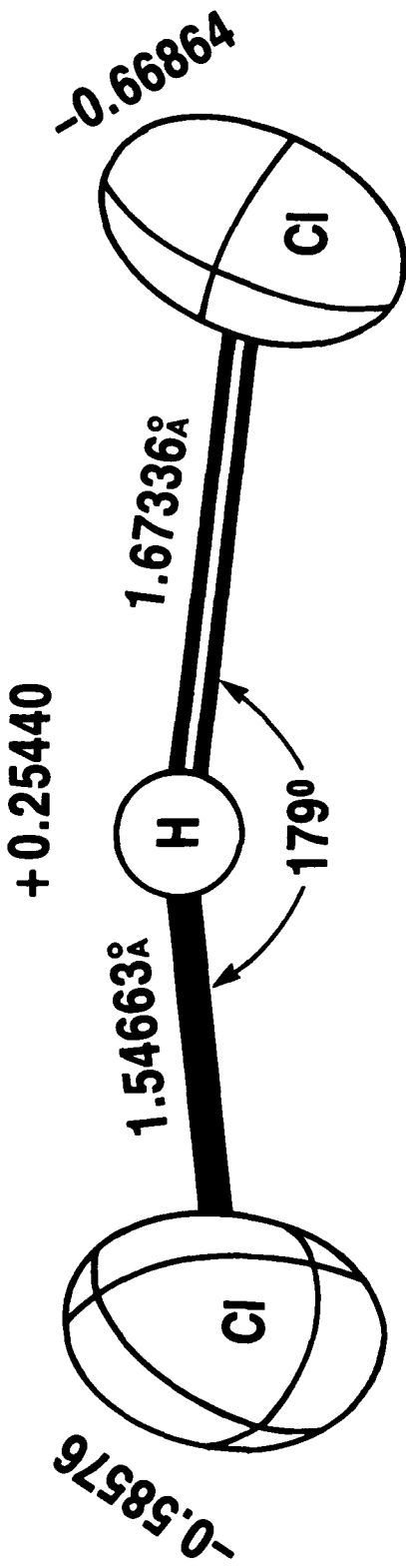


FIGURE 12. TEMPERATURE DEPENDENT CONDUCTANCE OF A 1:2 MELT:HCl SOLUTION.

Molecular Orbital Theory led by Professor Rodney Bartlet and has since conducted some M.O. calculations on  $[\text{HCl}_2]$  using a very sophisticated ab-initio procedure involving the use of Hartree-Fock (DZ) wave functions. He calculated that this species in question is stabilized by about 28 KCal per mole with respect to its constituents. Efforts are being made to establish the program at a UD computer. A thanks is due to the efficient computer staff at the OCA-Academic Services.

In some organic compounds containing  $[\text{HCl}_2]^-$  ion, the X-ray analysis showed the anion ( $\text{HCl}_2$ ) to be somewhat bent ( $\angle \text{Cl}-\text{H}-\text{Cl} = 168^\circ$ ) with unequal H-Cl bond distances (1.45 and 1.78 $\text{\AA}$ ). Our M.O. calculation with structure optimization, rather indicates a linear  $\text{HCl}_2$  moiety ( $\angle 179^\circ$ ) with unequal H-Cl bond lengths (1.55 and 1.67 $\text{\AA}$ ) (see Figure 13). Calculations of partial charges on the atoms definitely indicate charge separation with hydrogen being partially positive (+0.254). This is in accord with our observation of the downfield NMR shift of the  $\text{HCl}_2^-$  proton. Further calculations are in progress.

## Ab-initio Calculations



$\text{Cl} \cdots \text{Cl}: 3.21000\text{\AA}$

DICHLOROHYDROGEN (1) ION,  $\text{HCl}_2^-$

FIGURE 13. DICHLOROHYDROGEN(1) ION,  $\text{HCl}_2^-$ .

## SECTION 2

### PROTON NUCLEAR MAGNETIC RESONANCE AND RAMAN SPECTROSCOPIC STUDIES OF LITHIUM-WATER INTERACTIONS IN ACETONITRILE SOLUTIONS

#### 2.0 INTRODUCTION

Lithium has been used for many years as an anode material for non-aqueous batteries. Its large electrochemical potential, availability and cost have made it most attractive. The reactivity of the metal with organic solvents or their impurities has presented significant energy conversion problems. Passivated lithium causes a voltage delay when power is initially drawn and lasts until local heating at the electrode can dissipate the film. A thorough study of the reactivity of lithium metal using surface spectroscopic methods was reported recently. Information about the physical state of the lithium ion in solution has been gained from conductance and transference studies<sup>1</sup> of lithium salts in solution. A study of the coordination of lithium ion in solution presents a challenge because it is not a transition metal. Its large charge to volume ratio makes its chemistry a curiosity. Detailed knowledge of the electrochemical charge transfer process should include a study of the lithium ion environment.

#### 2.1 EXPERIMENTAL

##### 2.1.1 Materials

Most of the materials used in this study readily absorb atmospheric moisture. In order to minimize contamination by water, solutions were prepared under an atmosphere of argon in a glove box. The acetonitrile(AN) used in this study was HPLC grade, purchased from Burdick and Jackson. The AN as received was analyzed by passage through a capillary chromatograph(HP 5890) containing a (HP-101)non-polar methyl silicone fluid capillary

column. The only detectable impurity found was propionitrile.<sup>2</sup> The acetonitrile was further dried by passage and storage over activated alumina in a glove box. After solutions of lithium perchlorate in anhydrous acetonitrile were prepared, and determined to be free of water, desired quantities of water were added through a septum in the cap of the NMR tube.

Lithium perchlorate was purchased from Alfa Inorganics as the tri-hydrate salt, and was fused under vacuum in an all glass container immediately prior to solution preparation. The lithium perchlorate concentration of the solution was determined gravimetrically, by distilling the acetonitrile under vacuum from an aliquot of solution, followed by gently heating to 100°C and then weighing the residue.

**Caution:** Perchlorates, and particularly perchlorates in contact with organic solvents are potentially explosive. All solutions used in this study were prepared on as small a scale as possible in a glove box.

#### 2.1.2 Instrumental Methods

Proton NMR measurements were made using a Varian EM360L NMR spectrometer. Anhydrous solutions of lithium perchlorate in acetonitrile were placed in NMR tubes with screw-on caps and teflon septa. Water was added to these solutions using a microliter syringe.

Raman spectra were collected on the same solution as NMR measurements were made using a Spex Model 1688 analytical Raman system. The system is based on a computer controlled 0.25 M double spectrometer with photon counting detection. The light source for the Raman spectra was a Spectra Physics Model 2020 argon ion laser operating at 514 nm and a power at the sample of 100 mW. The spectrometer entrance and exit slits were set to 100 M.

Infrared spectra were collected using a Mattson Cygnus 100 FT-IR ( $0.125\text{ cm}^{-1}$  resolution) equipped with a water cooled source and MCT detector. Internal reflectance spectra were obtained using a 45 degree single reflection ZnSe prism mounted in a Harrick PLC-11M Prism Liquid Cell. Solution samples were loaded into the liquid cell inside the glove box, sealed and inserted into the spectrometer. The spectrometer was thoroughly purged with dry nitrogen prior to data collection. The identical procedure was followed to collect the background interferogram.

## 2.2 RESULTS AND DISCUSSION

### 2.2.1 Proton Nuclear Magnetic Resonance

The proton NMR spectrum of anhydrous acetonitrile shows a singlet at 1.98 ppm downfield from TMS. The proton NMR spectrum of acetonitrile, saturated with fused lithium perchlorate also shows only a singlet at 1.99 ppm from TMS. The small change in chemical shift can be attributed to the presence of lithium ion and the solvation of the ion by acetonitrile. The NMR of the lithium perchlorate solution however shows a peak at 1.99 ppm and a much second peak at 3.42 ppm.. The second smaller peak is indicative of a small amount of residual water within the system.

The subsequent addition of water to saturated solutions of lithium perchlorate in acetonitrile causes a second peak to be observed in the proton NMR spectrum which may be ascribed to the water protons. The chemical shift of the water protons and acetonitrile protons is shown in Table 1. The chemical shift of the second peak decreases slightly as water is added until the water to lithium ratio is approximately 1:1; remains constant until a water to lithium ratio of 4:1 is reached, at which time the chemical shift increases (Figure 1).

The observation that the chemical shift of the water protons in acetonitrile solution through the addition of a

TABLE 1  
CHEMICAL SHIFT DATA FOR LITHIUM PERCHLORATE SOLUTIONS  
IN ACETONITRILE AS A FUNCTION OF ADDED WATER

<u>L Water Added</u>	<u>[H<sub>2</sub>O] [Li+]*</u>	<u>CH<sub>3</sub> Chemical Shift (Hz)</u>	<u>H<sub>2</sub>O Chemical Shift (Hz)</u>
0.5	0.04	120	210
1.0	0.07	120	210
2.0	0.13	119	209
5.0	0.33	119	208
10.0	0.66	119	208
15.0	0.98	119	206
20.0	1.31	120	205
25.0	1.64	120	205
30.0	1.96	120	205
35.0	2.28	120	205
40.0	2.61	119	205
45.0	2.94	119	205
50.0	3.27	120	205
55.0	3.60	119	205
60.0	3.92	120	205
65.0	4.25	121	206
75.0	4.91	119	207
85.0	5.55	120	209
95.0	6.21	121	211
115.0	7.52	122	215

\* The initial lithium ion concentration in these solutions was 1.6 M

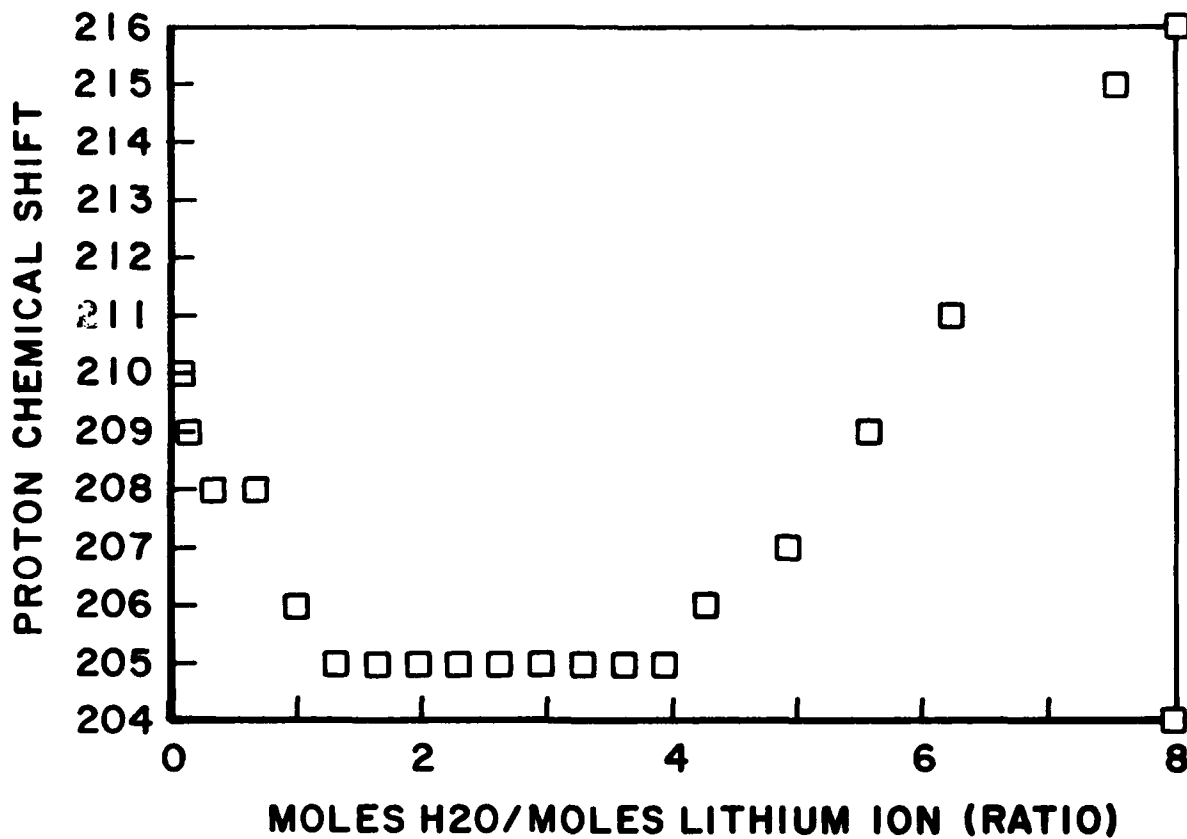


FIGURE 14. CHEMICAL SHIFT (Hz) AT 60 MHz OF WATER PROTONS AS A FUNCTION OF MOLE RATIO, WATER:LITHIUM ION, IN ACETONITRILE.

large amount of water is in contrast with NMR data for solutions without added lithium ion. The data indicates that water is not simply an added component in the solvent but that the water is bound to the lithium ion in solution. The data presented in Figure 1 and Table 1 suggests that as water is added to the solution of lithium perchlorate in acetonitrile, the water is incorporated into the coordination sphere of the lithium ion. After the coordination sphere of the lithium ion is filled, then excess water is in rapid equilibrium between the lithium coordination sphere and the bulk of the solution. In this case the chemical shift is the average between the two separate species in rapid equilibrium.

### 2.2.2 Raman Spectroscopy

The Raman spectrum of lithium perchlorate shows a splitting of carbon-nitrogen stretching vibration at 2249  $\text{cm}^{-1}$  into bands at 2249 and 2270  $\text{cm}^{-1}$ . The band at 2270  $\text{cm}^{-1}$  can be attributed to the formation of a lithium acetonitrile complex in solution. Other vibrational bands in the acetonitrile spectrum change very little with the addition of lithium perchlorate, consistent with previous observations.<sup>3</sup>

The addition of water to saturated solutions of lithium perchlorate in acetonitrile brings about a decrease in the vibrational band at 2270  $\text{cm}^{-1}$  as shown in Figure 2. The decrease in intensity is believed due to the displacement of acetonitrile from the coordination sphere of the lithium ion by the added water. Other changes which are observed in the Raman spectra of these solutions include a broadening of the vibrational band at 2249  $\text{cm}^{-1}$  and the appearance of bands around 3500  $\text{cm}^{-1}$  and 1800  $\text{cm}^{-1}$ . As the ratio of moles of water to moles of lithium ion approaches 4:1, the energy of the vibrational band at 2270  $\text{cm}^{-1}$  decreases slightly as the intensity decreases. When the ratio of water to lithium ion is four or above, the band at 2270  $\text{cm}^{-1}$  is almost completely absent.

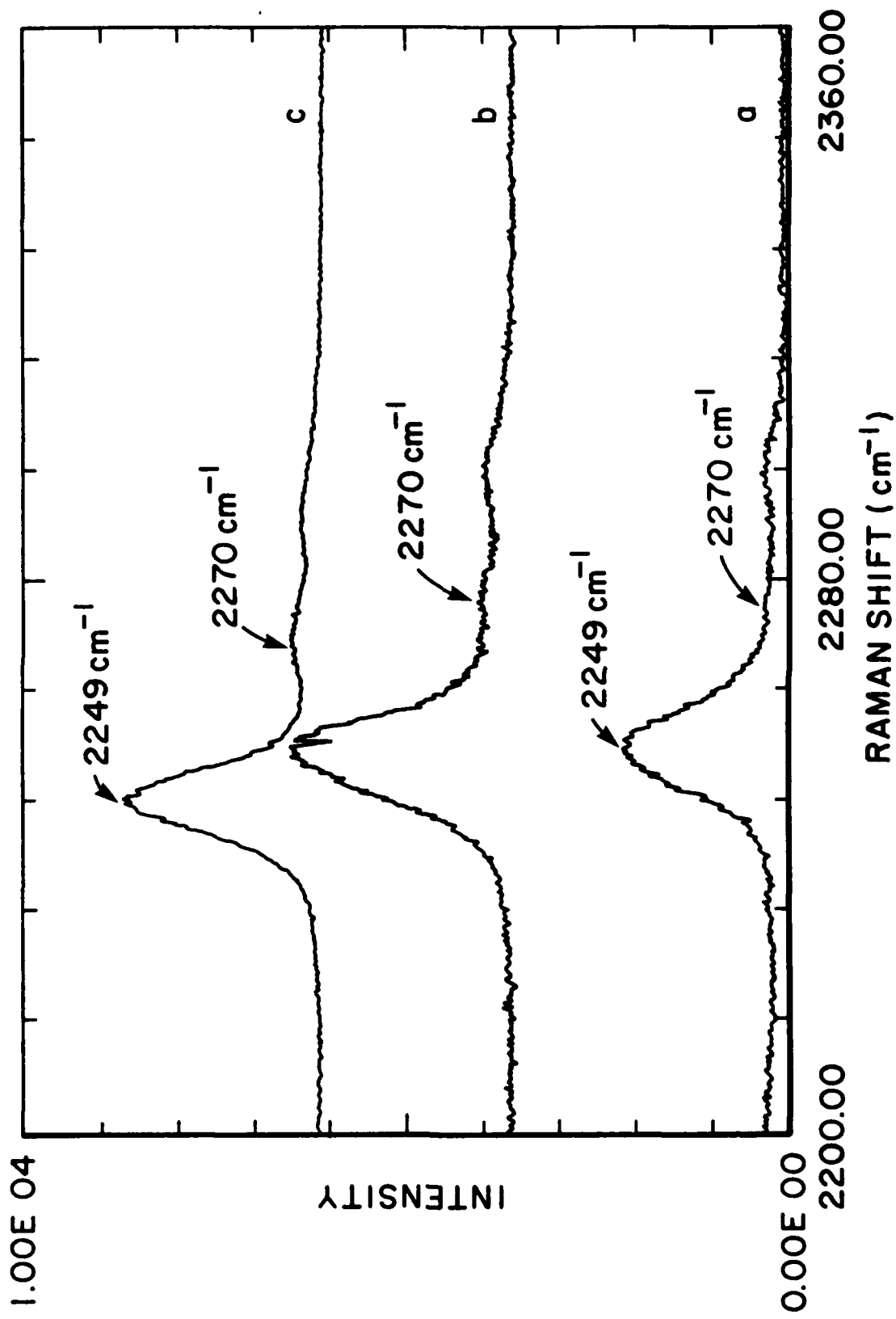


FIGURE 15. RAMAN SPECTRA OF LITHIUM PERCHLORATE(1.6 MOLAR) IN ACETONITRILE:  
 (a) NO ADDED WATER, (b) WATER:Li<sup>+</sup> MOLAR RATIO 1.5:1; (c) WATER:Li<sup>+</sup>  
 MOLAR RATIO, 4:1.

The observations in the Raman spectra suggest that water preferentially displaces acetonitrile from the lithium ion. In previous work on other solvent such as tetrahydrofuran, water was found to displace the solvent from the lithium ion. When the Raman evidence is coupled with NMR results they suggest that water effectively displaces acetonitrile until a complex of the form  $\text{Li}(\text{H}_2\text{O})_4^+$  is formed.

#### 2.2.3 Infrared Spectroscopy

The infrared spectra of lithium perchlorate in acetonitrile have many of the same features as the Raman spectra (Figure 3). The major differences are in the intensities of the various features. The absorption band at  $2270 \text{ cm}^{-1}$  is much more intense in the infrared than in the Raman.

The addition of water to these solutions decreases the intensity of the absorption at  $2270 \text{ cm}^{-1}$  and brings about a very noticeable broadening of the  $2249 \text{ cm}^{-1}$  band. The  $2270 \text{ cm}^{-1}$  band does not completely disappear from the infrared spectrum as it does in the Raman spectrum. Both of these observations are indicative of the displacement of acetonitrile from the first coordination shell of the lithium ion.

The infrared data suggest that the displacement of acetonitrile from the coordination sphere is not complete, but some acetonitrile remains within the coordination sphere of the lithium ion. The broadening of the infrared band at  $2249 \text{ cm}^{-1}$  can be attributed to hydrogen bonding between acetonitrile and water present in solution.

### 2.3 SUMMARY AND CONCLUSIONS

The interactions between lithium ion and water in acetonitrile solution have been investigated using proton nuclear magnetic resonance, infrared and Raman spectroscopies. The

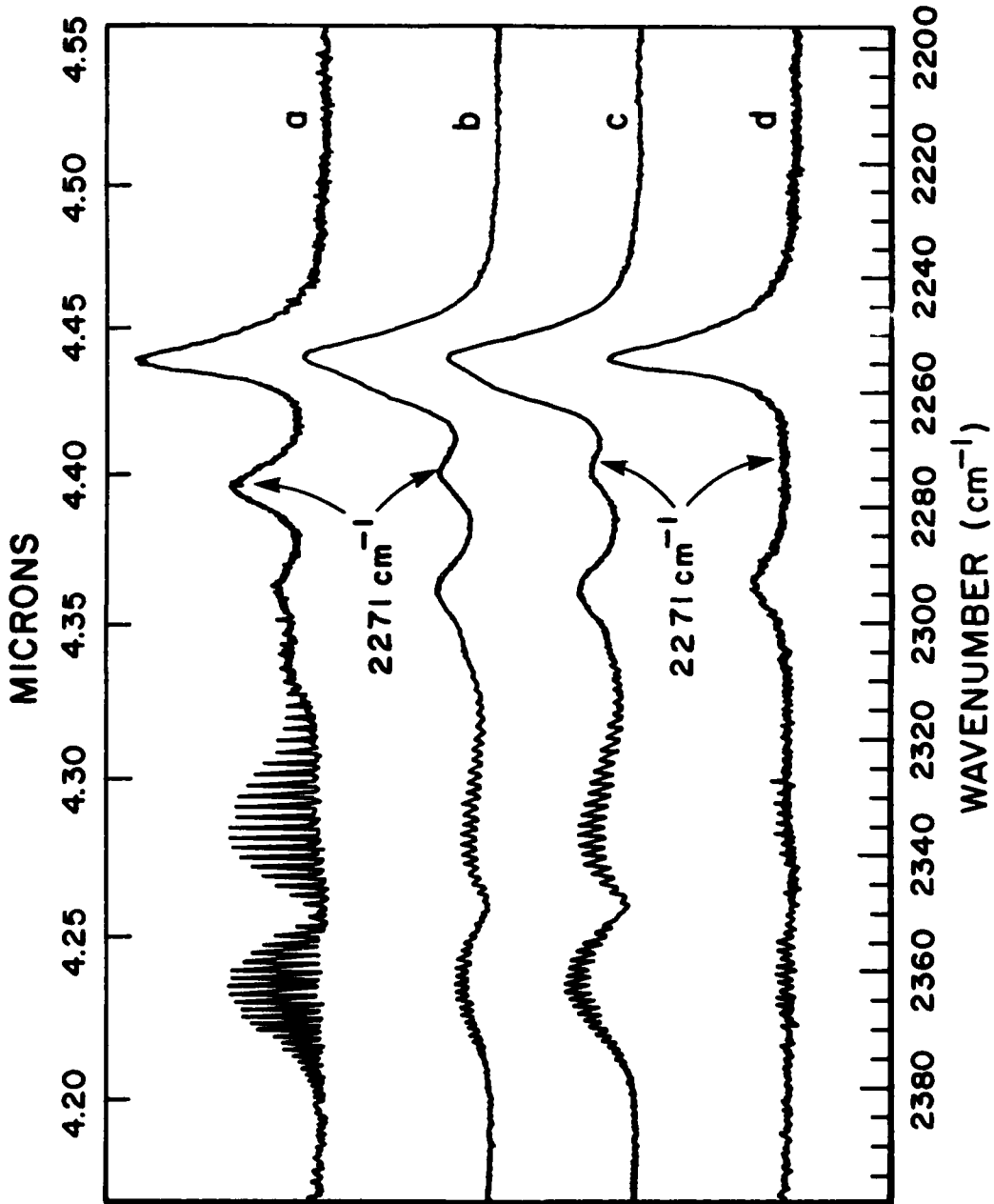


FIGURE 16. INFRARED SPECTRA OF LITHIUM PERCHLORATE (1.6 MOLAR) IN ACETONITRILE CONTAINING VARIOUS AMOUNTS OF WATER: (a) NO ADDED WATER, (b) 5.0 MOLAR WATER, (c) 7.0 MOLAR WATER; (d) NO ADDED WATER, NO  $\text{LiClO}_4$  NEAT ACETONITRILE.

chemical shift of the water protons in the acetonitrile solutions of lithium ion remains constant until the molar ratio of water to lithium ion equals 4. Additional quantities of water cause the chemical shift of the water peak to increase. Infrared and Raman spectra show a decrease in the intensity of vibrational band at  $2270\text{ cm}^{-1}$  as water is added. This vibrational band is ascribed to the effect solvation has upon the cyanide stretching frequency. In addition to a decrease in intensity of the vibrational bands, a shift to lower energy is observed as water is added. This data suggests that water displaces acetonitrile from the lithium ion until a four coordinate complex between lithium ion and water is formed.

#### 2.4 REFERENCES

1. Venkatasetty, H. V., *Lithium Battery Technology*, The Electrochemical Society Monograph Series, Pennington, New Jersey, 1984.
2. Russo, B., Senior Thesis, "Gas Chromatographic Analysis of Impurities in Organic Solvents," Chemistry Department, University of Dayton, Dayton, Ohio, 1988.
3. Cotzee, J. F. and W. R. Sharpe, J. Solution Chem., 1, 1972, p. 77.

### SECTION 3

#### A GAS CHROMATOGRAPHIC STUDY OF THE REACTIVITY OF LITHIUM WITH ACETONITRILE

##### 3.0 INTRODUCTION

This research concerns the reaction of acetonitrile(AN) with lithium metal, the reaction products formed and postulating a possible mechanism for the reaction. The first part of the research emphasized the identification of acetonitrile and impurities present by the capillary chromatography method.<sup>1</sup> The second part dealt with the kinetics of the reaction and the identification of product(s) formed. A mechanism for the reaction was developed based on observations of physical changes which occur during the course of the reaction. Acetonitrile is a widely used organic solvent for electrochemical studies because of its physical properties and because it is stable over a wide range of potentials.<sup>2</sup> Its usefulness, as a solvent, may be compromised by the presence of impurities. Herbert Keisele reported that there generally exist six major impurities in AN:<sup>3</sup> allyl alcohol, benzene, methanol, acrylonitrile, propionitrile and water. After purification, propionitrile is the only impurity remaining in a measurable amount.

Gas chromatography is a technique for separating volatile substances by passing a gas stream over a stationary phase.<sup>4</sup> In the last several years, the gas chromatography technique has had a great demand in the analysis of polymers for industry. Its preference over other techniques such as thin-layer chromatography and liquid chromatography, is due to the fact that gas chromatography is ideally suited for the separation and quantification of component fractions.<sup>5</sup>

In recent work,<sup>6</sup> the electrolysis of solution of lithium perchlorate, in AN, resulted in the formation of polyindene in anode compartment of a divided cell. With no electrical current, the same solution formed no polymer.

### 3.1 EXPERIMENTAL

All reagents were kept inside a dry box filled with dry argon gas to avoid contamination. AN was treated with a large excess and then stored over alumina (Acid type WA-4) to remove water. The liquid reagents used in our work were HPLC quality and the lithium used was 99.9+ (metallic purity).

A Hewlett-Packard 5890 fused column capillary action Gas Chromatography and a non-polar HP-101 (Methyl Silicone Fluid 25m \* 0.32mm \* 0.03 $\mu$ m film thickness) capillary column were used. A Hamilton 1 $\mu$ L syringe was used to inject the samples. Unless otherwise indicated, the following operating conditions were maintained: Oven Temperature, 40°C; Injector and Detector Temperatures, 250°C; carrier gas and flow rate, helium at 100ml/min; Column Head Pressure, 10 psi; time, 6 min.; Attenuation, 2°; Range, 2<sup>7</sup>; Sample Volume, 0.45 $\mu$ L. A Hewlett-Packard 3390A Integrator was used to record the chromatograms at an attenuation of 2°. The first step was to determine the retention times of pure AN and propionitrile using the same experimental conditions. Several samples of AN were transferred to vials inside the dry box, removed, and chromatograms obtained. We also studied the reaction of AN and lithium metal. Masses of lithium metal were added to a constant volume of AN. Following the addition of lithium, the physical changes were noted. The temperature was controlled by refrigeration at a temperature of 6-8°C. Samples were centrifuged to precipitate high molecular weight material prior to obtaining the chromatograms.

### 3.2 RESULTS

Keisele reported a procedure to remove six major contaminants from AN. HPLC quality AN contains only one contaminant in measurable amount. Figure 1A shows the chromatogram obtained for AN - two peaks with different retention times and area percentages are observed. To identify each peak in our chromatograms (Table 1), the following steps were followed:

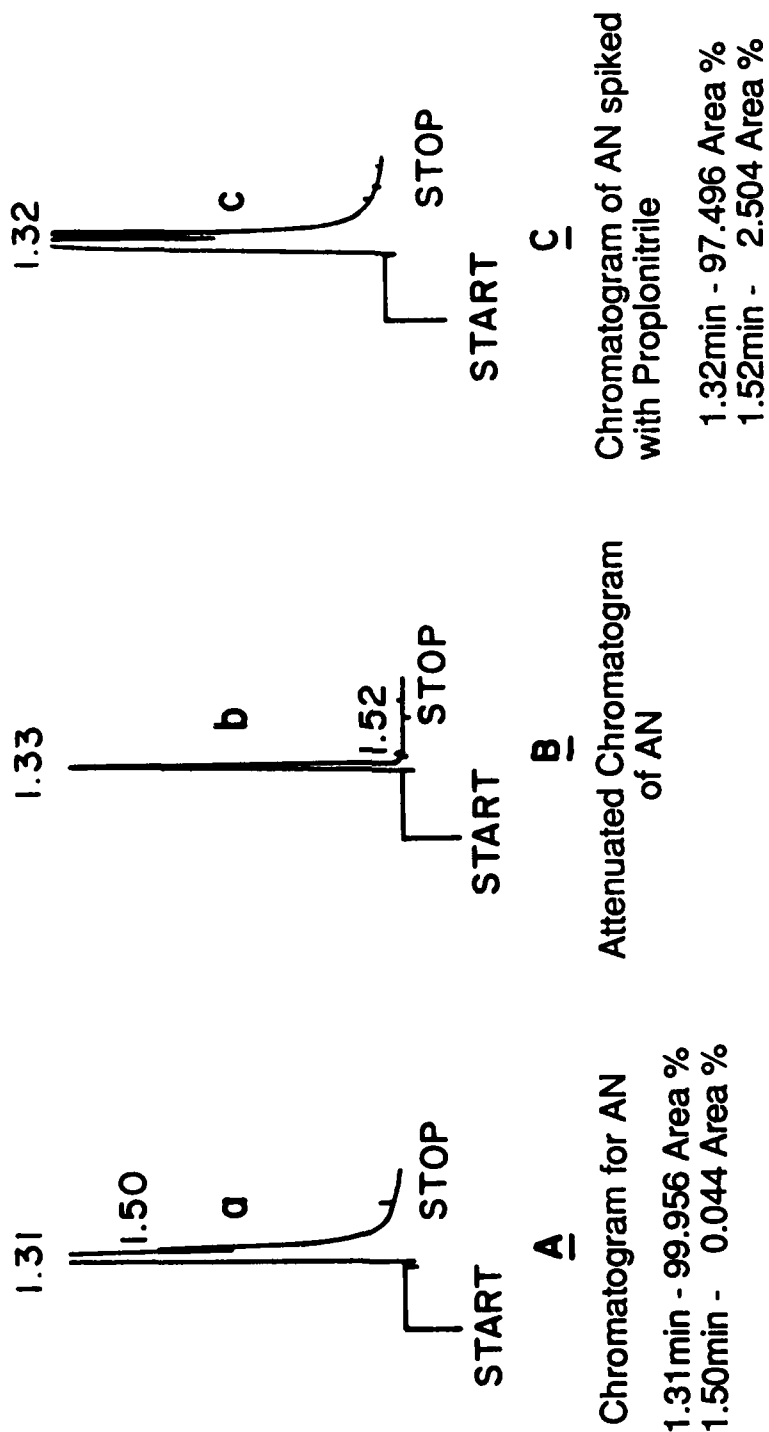


FIGURE 17. GAS CHROMATOGRAMS OF ACETONITRILE: (a) NORMAL, (b) ATTENUATED, (c) SPIKED WITH PROPIONITRILE.

TABLE 1  
RETENTION TIMES OF ACETONITRILE AND PROPIONITRILE

<u>Figure 1</u>	<u>ACETONITRILE</u>		<u>PROPIONITRILE</u>	
	<u>Retention Time (min)</u>	<u>Area %</u>	<u>Retention Time (min)</u>	<u>Area %</u>
A	1.32	99.956	1.51	0.044
B	1.33	99.957		
C	1.33	97.432	1.53	2.568

TABLE 2  
AREA PERCENTAGE VALUES OF THOSE MAJOR PEAKS  
FROM THE REACTION SAMPLES 1, 2, 3, 4

<u>Reaction Sample</u>	<u>Retention Time (min)</u>	Area Percentage (%)		
		<u>Initial</u>	<u>Middle</u>	<u>Final</u>
1	1.18-1.22	0.117	0.189	0.002
	1.29-1.36	9.137	47.627	1.878
	1.39-1.43	99.877	52.301	26.694
	1.49-1.52	98.120	88.123	98.122
2	1.19-1.22	0.008	0.059	0.005
	1.32-1.36	26.747	29.600	8.236
	1.46-1.49	59.188	73.153	91.739
3	1.18-1.21	0.028	0.065	0.010
	1.30-1.34	22.496	53.195	17.212
	1.38-1.43	99.649	59.395	43.323
	1.47-1.50	82.759	20.804	60.913
4	1.19-1.22	0.016	0.057	0.010
	1.32-1.36	52.153	90.195	50.403
	1.38-1.41	9.557	52.668	8.491
	1.49-1.52	58.001	70.763	32.094

- (a) An attenuated chromatogram of AN was obtained (Figure 1B). The increase in attenuation causes the disappearance of all other peaks except the one corresponding to the solvent.
- (b) AN does contain one impurity, propionitrile. A sample of AN spiked with propionitrile was then prepared and a chromatogram obtained (Figure 1C). When the solvent is spiked with propionitrile, the area percentage and the height of the peak at the same retention time increases.

The physical changes observed for each of the reactions of AN and lithium metal were consistent throughout. The reaction started immediately after the AN was added to the piece of lithium metal in the vial. Tiny bubbles around the piece of lithium metal and a white precipitate having the appearance of small cotton "mobs" formed a short time after the addition of lithium. The lithium becomes coated with a white "passivating" layer. There is no doubt that it is AN which reacts with lithium even after being coated with a film which is partially protective. At this point, precipitate formation appears to cease, and the solution begins to exhibit a light green color.

The pressure, due to the gaseous reaction products, becomes appreciable within the reaction tube. The larger the mass of lithium metal used the better one is able to see the change in color of the solvent - from a clear to a light green color, which will turn to an even darker color as the reaction progresses.

The precipitate has a different consistency; it is "gooey" - and as bubbles (or the polymer) are formed it shoots off from the surface. The volume of the polymeric material increases as the reaction progresses and depending on the mass of lithium metal used, the reaction medium becomes more viscous until no more bubbles come from the gooey precipitate. This last

observation indicates that the polymerization is reaching termination.<sup>7</sup> The final color of the reaction is now dark yellow-orange color. The only difference between experiments was that as the mass of lithium metal increases the reaction velocity increases. As the mass of lithium metal was increased, the temperature of the vial increased also, in spite of the fact that the reaction was thermostatically controlled. The mass of lithium metal added to 2.0 mL of AN varied from 0.0048 to 0.0404 grams.

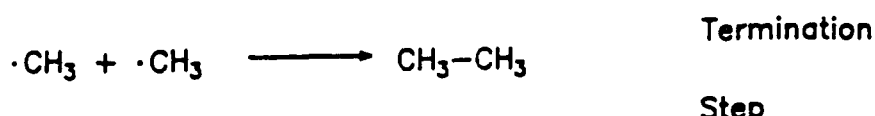
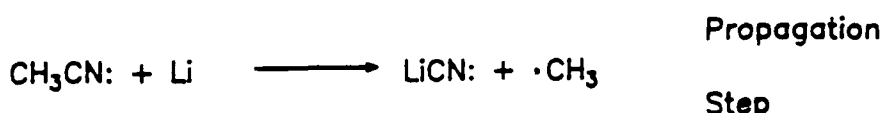
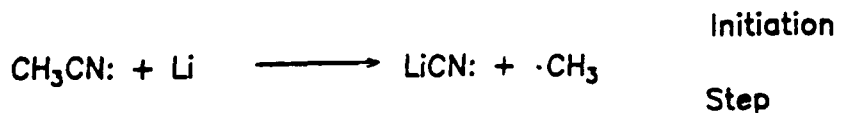
It has been reported that nitriles undergo polymerization with ionic catalysts on rare occasions. Kabanov<sup>8</sup> studied the polymerization of nitriles by monitoring the infrared spectrum of the reaction as a function of time. The spectra of the nitrile solvent was done first to identify the CN peak which has a wave number of  $2240\text{ cm}^{-1}$ . The trimer and the polymer spectra were done next. We found that the CN peak was no longer present in the trimer spectra, instead an "intense band at  $1606\text{ cm}^{-1}$ , probably corresponding to conjugated C=N bond" was now present in the spectrum of high polymer. These results are consistent with other complex nitrile reactions studied.<sup>8</sup>

Based on the information collected and the physical changes observed during the reaction, a possible mechanism for the reaction of AN and lithium metal is suggested (Figure 2). The reaction can follow either of two paths, each one giving different reaction products:

- (1) One reaction product can be ethane. It is known that ethane gas is formed when methyl radicals react;
- (2) The other reaction product is the polymer. First, the reaction gives a free radical containing the conjugated form of the nitrile triple bond - C=N. This is the monomer of the polymer. When the radical reacts with another molecule of AN and repeated, the result will be polymerization.

## POSSIBLE MECHANISM FOR LITHIUM-ACETONITRILE REACTION

### A. Ethane



### B. Polymer

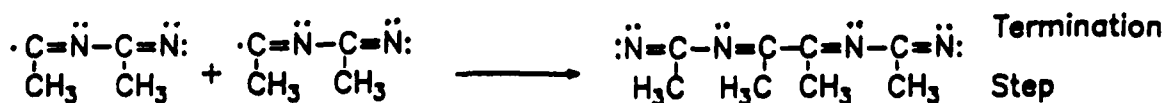
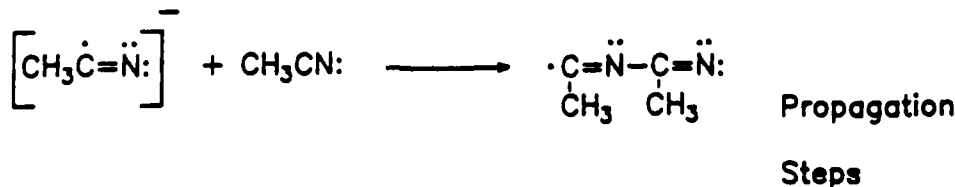
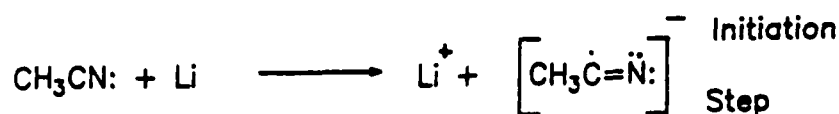


FIGURE 18. PROPOSED MECHANISM FOR THE CHEMICAL REACTION BETWEEN LITHIUM AND ACETONITRILE.

Chromatograms from the reactions of AN and lithium metal yield four peaks: (a) 1.18-1.22 min., (b) 1.30-1.36 min., (c) 1.40-1.43 min., and (d) 1.49-1.55 min. The attenuation of the integrator and gas chromatography was increased from initial values of  $2^{\circ}$  to  $2^{4-7}$  and  $2^3$ , respectively; to obtain optimal peak separation. Figures 2A through 2D show the chromatograms obtained 3 hours and 50 minutes after commencement of each reaction.

We found that the retention time for AN equals 1.32-1.33 min. under these experimental conditions and that the area percentage was approximately 99.956%. We assume that when lithium metal begins to react with AN, the possibility of a shift in retention time for the major peak owing to the physical and chemical changes exists and that the area percentage of the AN peak is going to decrease. The magnitude of the chromatographic peaks reach their maximum values at a point in time after the reaction has begun but is far from complete (Table 2). It is probable that those peaks found in the range of 1.30-1.36 min. of the chromatograms can be assigned to AN. Individual retention times and area percentages are not presented because approximately 40 chromatograms were obtained for each reaction.

A major problem encountered is the range of values obtained for the area percentages of each peak necessary to identify the possible reaction products. For example, the peak with a retention time of approximately 1.20 min., started with a small value of area percentage (Table 2). We assume that the area percentage is going to decrease as the reaction progresses because the peak was not present in the chromatogram obtained for AN at the beginning of the study. Therefore, our first assumption is that the peak is that of a reaction product. We found that the area percentage of the peak not only increases but then actually decreases toward termination of the reaction. Similar results were obtained for other peaks, but not as dramatic (Table 2).

The day after each reaction reached termination, a chromatogram was obtained and compared with existing data. The first observation made was that the peak at 1.20 min. was no longer present and is assumed not to be a major product of the reaction. However, the area percentages of the 1.5 min. peak decreased as the mass of lithium metal was increased. It may be postulated that this product at that retention time is an intermediate, since it gradually disappeared. A definitive conclusion might have been possible had additional data been taken and had the temperature been maintained constant during the course of the reaction. The peak that might be AN, at a retention time of approximately 1.30-1.36 min. was significant only in the chromatogram of the second reaction sample. No conclusions can be drawn from this observation because there was no way to follow the reaction from its commencement (Table 3).

### 3.3 CONCLUSIONS

From the results of the reaction of lithium with AN, we postulate that lithium metal reacts with AN to yield a polymer and a gas. The polymerization process involves the generation of reaction intermediates, which we can see using capillary chromatography. The peaks, because of these intermediate species, decrease as the polymerization process continues.

### 3.4 REFERENCES

1. Russo, B., "Gas Chromatographic Analysis of Impurities in Organic Solvents," Bachelor's Thesis, University of Dayton, April, 1988.
2. Fry, Albert J. and Wayne F. Britton, "Solvents and Supporting Electrolytes," in Laboratory Techniques in Electro-Analytical Chemistry, Peter T. Kissinger and William R. Heineman, eds., (New York: Marcel Dekker, 1984), p. 371.
3. Keisele, Herbert, "Purification of Acetonitrile," Analytical Chemistry, 52, (1980), p. 2230.

TABLE 3

RETENTION TIMES (RT) AND AREA PERCENTAGE (A%)  
OBSERVED THE DAY AFTER REACTION REACHED TERMINATION

SAMPLE	REACTION	1	2	3	4	
	RT	A%	RT	A%	RT	A%
		1.14	0.051			
				1.21	0.009	
		1.33	86.065			
1.40	27.845	1.43	13.582	1.39	56.802	
1.53	72.064			1.49	43.189	1.51
						21.330

4. McNair, H. M. and E. J. Bonelli, Chapter 1 - Introduction in Basic Gas Chromatography, (1968), p.1.
5. Sullivan, J. F., Chapter 14 - Polymer Analysis Using Gas Chromatography in Modern Practice of Gas Chromatography, R. L. Grob, ed., Second Edition, (John Wiley and Sons, 1985) p. 722.
6. Kikuchi, Yasuo and Hiroshi Fukuda, "Electrochemical Polymerization of Indene," Journal of Polymer Science, Vol. 11, No. 10, (1973), p. 2709.
7. Eastmond, G. C., Chapter 1 - The Kinetics of Free-Radical Polymerization of Vinyl Monomers in Homogeneous Solutions, in Comprehensive Chemical Kinetics, Vol. 14A - "Free Radical Polymerization," C. H. Bamford and C. F. H. Tipper eds., (Amsterdam: Elsevier Sceintific Publishing Co., 1976), p. 76.
8. Kabanov, V. A., V. P Zubov, V. P. Kovaleva, and V. A. Kargin, "Polymerization of Nitriles and Pyridine," Journal of Polymer Science: Part C, (1964) p. 1009.